Postnatal Cardiac Gene Editing Using CRISPR/Cas9 With AAV9-Mediated Delivery of Short Guide RNAs Results in Mosaic Gene Disruption

Anne Katrine Johansen, Bas Molenaar, Danielle Versteeg, Ana Rita Leitoguinho, Charlotte Demkes, Bastiaan Spanjaard, Hesther de Ruiter, Farhad Akbari Moqadam, Lieneke Kooijman, Lorena Zentilin, Mauro Giacca, Eva van Rooij

Rationale: **CRISPR/Cas9 (clustered regularly interspaced palindromic repeats/CRISPR-associated protein 9)–based DNA editing has rapidly evolved as an attractive tool to modify the genome. Although CRISPR/Cas9 has been extensively used to manipulate the germline in zygotes, its application in postnatal gene editing remains incompletely characterized.**

Objective: **To evaluate the feasibility of CRISPR/Cas9-based cardiac genome editing in vivo in postnatal mice.**

Methods and Results: **We generated cardiomyocyte-specific Cas9 mice and demonstrated that Cas9 expression does not affect cardiac function or gene expression. As a proof-of-concept, we delivered short guide RNAs targeting 3 genes critical for cardiac physiology, *Myh6*, *Sav1*, and *Tbx20*, using a cardiotropic adeno-associated viral vector 9. Despite a similar degree of DNA disruption and subsequent mRNA downregulation, only disruption of *Myh6* was sufficient to induce a cardiac phenotype, irrespective of short guide RNA exposure or the level of Cas9 expression. DNA sequencing analysis revealed target-dependent mutations that were highly reproducible across mice resulting in differential rates of in- and out-of-frame mutations. Finally, we applied a dual short guide RNA approach to effectively delete an important coding region of *Sav1*, which increased the editing efficiency.**

Conclusions: **Our results indicate that the effect of postnatal CRISPR/Cas9-based cardiac gene editing using adeno-associated virus serotype 9 to deliver a single short guide RNA is target dependent. We demonstrate a mosaic pattern of gene disruption, which hinders the application of the technology to study gene function. Further studies are required to expand the versatility of CRISPR/Cas9 as a robust tool to study novel cardiac gene functions in vivo. (*Circ Res*. 2017;121:1168-1181. DOI: 10.1161/CIRCRESAHA.116.310370.)**

Key Words: clustered regularly interspaced short palindromic repeats ■ gene editing ■ molecular biology ■ myocytes, cardiac ■ sequence analysis, DNA

Downloaded from http://circres.ahajournals.org/ by guest on February 6, 2018

Genetic engineering of mammalian species, in particular *Mus musculus*, has answered fundamental questions related to basic biology and disease. Traditionally, this has heavily relied on the generation of genetically modified mice by transgenesis or gene targeting in embryonic stem cells. However, the generation of transgenic mice is a time consuming, expensive process, and requires a substantial number of animals.[1,2] Although spatiotemporally controlled models using tetracycline-dependent transactivators or tamoxifen-inducible recombinases have proven effective for studying gene function postnatally, these models have important limitations inherent to the drugs used to activate/deactivate gene expression or induce LoxP-mediated recombination.[3,4]

Editorial, see p 1111
In This Issue, see p 1103
Meet the First Author, see p 1104

The discovery that the *Streptococcus pyrogenese* clustered regularly interspaced palindromic repeats (CRISPR)-associated (Cas9) endonuclease can be redirected to induce DNA double-strand breaks (DSBs) within specific genomic loci has revolutionized the way animal models can be generated. Cas9 target activity relies on precise RNA–DNA base pairing between (1) the engineered short guide RNA (sgRNA) with the target DNA strand[5] and (2) through interactions with the nontarget DNA strands protospacer-adjacent motif and the protospacer-adjacent motif interaction motif in Cas9.[6] The

Original received November 27, 2016; revision received August 24, 2017; accepted August 29, 2017. In July 2017, the average time from submission to first decision for all original research papers submitted to *Circulation Research* was 12.80 days.

From the Hubrecht Institute, Royal Netherlands Academy of Arts and Sciences (A.K.J., B.M., D.V., A.R.L., C.D., B.S., H.d.R., F.A.M., L.K., E.v.R.) and Department of Cardiology (D.V., C.D., E.v.R.), University Medical Center Utrecht, The Netherlands; and International Centre for Genetic Engineering and Biotechnology, Trieste, Italy (L.Z., M.G.).

The online-only Data Supplement is available with this article at http://circres.ahajournals.org/lookup/suppl/doi:10.1161/CIRCRESAHA.116.310370/-/DC1.

Correspondence to Eva van Rooij, PhD, Molecular Cardiology, Hubrecht Institute for Developmental Biology and Stem Cell Research, Royal Netherlands Academy of Arts and Sciences (KNAW), 3584 CT Utrecht, The Netherlands. E-mail e.vanrooij@hubrecht.eu

© 2017 American Heart Association, Inc.

Novelty and Significance

What Is Known?

- Genome editing is being used increasingly to study gene function.
- CRISPR/Cas9 (clustered regularly interspaced palindromic repeats/CRISPR-associated protein 9) is a powerful tool that can be used to modify eukaryotic DNA in vivo.

What New Information Does This Article Contribute?

- Adeno-associated virus–mediated delivery of a short guide RNA targeting a specific gene in transgenic mice expressing Cas9 protein in cardiac myocytes postnatally results in a mosaic pattern of cardiac gene disruption.
- The phenotypic effect of mosaic gene disruption in the heart is target gene dependent.
- Using 2 separate short guide RNAs against the same gene in parallel mediates precise genome editing and improves targeting efficiency.

The emergence of CRISPR/Cas9 as a tool to modify the eukaryotic DNA permanently has had a high impact on scientific research. Nevertheless, few studies to date have reported the application of CRISPR/Cas9 in gene modifications postnatally in the heart. This opportunity is appealing because it is faster and easier than conventional gene targeting approaches. Here, we used adeno-associated virus 9–mediated delivery of single short guide RNAs targeting 3 well-characterized cardiac genes, *Sav1*, *Tbx20*, and *Myh6* in cardiomyocyte-specific Cas9-expressing mice. By integrative protein, RNA, and DNA analyses, we detected a mosaic pattern of gene disruption. Induction of a cardiac phenotype on gene targeting in a subset of cardiomyocytes is target gene dependent. The application of a dual short guide RNA strategy mediates precise genome editing and improves the efficiency of target gene disruption. Our data highlight important limitations of the CRISPR/Cas9 system to study genes in the postnatal heart. However, the approach does offer the opportunity for mosaic gene analysis in a native environment.

Nonstandard Abbreviations and Acronyms

AAV9	adeno-associated virus serotype 9
Cas9	CRISPR-associated protein 9
CRISPR	clustered regularly interspaced palindromic repeats
DSB	double-strand break
eGFP	enhanced green fluorescent protein
Indels	insertion deletions
Myh6/7	myosin heavy chain 6/7
OT	off-target
Sav1	salvador 1
sgRNA	short guide RNA
Tbx20	T-box 20
T7E1	T7 endonuclease 1

DNA DSBs introduced by Cas9 are predominantly repaired by nonhomologous end joining. This is an error-prone process that randomly inserts or deletes nucleotides (indels), often introducing a frame-shift mutation resulting in the generation of a premature stop codon and thus inactivation of gene function.[7,8]

Elegant studies have recently used CRISPR/Cas9 to edit genes in vivo in the mouse liver,[9,10] lung,[11,12] heart,[13–15] skeletal muscle,[16–18] and brain.[19] However, a broader in-depth evaluation of the application of CRISPR/Cas9 to study the function of genes postnatally in the heart is currently lacking.

Here, we evaluated the efficiency of CRISPR/Cas9-mediated gene editing to study cardiac gene function in vivo using systemic and local delivery of sgRNAs. We present unexpected limitations of CRISPR/Cas9-based cardiac genome editing by showing inefficient gene disruption using adeno-associated virus serotype 9 (AAV9)–incorporated sgRNA delivery in cardiomyocyte-specific Cas9-expressing mice. Our data suggest that viral delivery of single sgRNAs introduces a low level of gene disruption in a mosaic fashion. Although this is sufficient for the disruption of some genes, for many genes, it presents an important limitation of using CRISPR/Cas9-based gene editing to study gene function in the heart. Finally, we show that removing a critical coding exon using a dual sgRNA approach demonstrates a more efficacious methodology to edit DNA.

Methods

Please refer to the Materials and Methods Section I in the Online Data Supplement for a detailed description of experimental methods.

Animals

All experiments were performed in accordance with the guidelines of the Animal Welfare Committee of the Royal Netherlands Academy of Arts and Sciences. To generate an organ-restricted Cas9 mouse, homozygous Cre-dependent Rosa26-Cas9 mice (B6;129-Gt(ROSA)26Sortm1(CAG-cas9*,-EGFP)Fezh/J; stock number 024857, obtained from Jackson Labs, Germany, which were originally generated on a C57/BL6N background) were crossed with myosin heavy chain 6 (*Myh6*)-Cre transgenic mice (Cre expression driven by a cardiomyocyte-specific promoter; a generous gift from Jeffery Molkentin, Cincinnati Children's Hospital Medical Center; bred on a C57/BL6N background) to generate $Myh6^{Cas9}$ mice. For all experiments, Cre-negative littermates were used as a control.

To generate transgenic mice with Cas9 expression driven by the cardiomyocyte-specific Myh6 promoter, we polymerase chain reaction (PCR) amplified 3XFLAG-Cas9 from the plasmid pX330-U6-Chimeric_BB-CBh-hSpCas9, a gift from Feng Zhang (Addgene plasmid no. 42230), using primers with added *Sal*I and *Hin*dIII restriction sites (see Section II in the Online Data Supplement for primer sequences). The resulting product was purified and inserted into *Sal*I- and *Hin*dIII-digested pJG/Myh6, a gift from Jeffrey Robbins. The *Myh6*-3XFLAG-Cas9 plasmid was linearized, purified, and injected into zygotes of F_1 C57/BL6/CBA mice.

sgRNA Design

We designed sgRNAs for SpCas9 target selection using the CRISPR design tool (http://crispr.mit.edu/), which systematically screens for off-target (OT) effects.[20] The 20-nucleotide sequences were designed to precede a CRISPR type II–specific protospacer-adjacent motif sequence 5′–NGG. sgRNA sequences are listed in Section II in the Online Data Supplement.

Downloaded from http://circres.ahajournals.org/ by guest on February 6, 2018

sgRNA Constructs, Transfection, and T7 Endonuclease 1 Assays

Single-stranded sgRNA sequences were annealed and cloned into pSpCas9(BB)-2A-Puro (PX459) after restriction digestion with *Bbs*1 (PX459 was a gift from Feng Zhang [Addgene plasmid no. 48139]).[21] Successful cloning was confirmed by double digestion with *Bbs*I and *Age*I. To determine functionality of sgRNA, sgRNA-PX459 vectors were transfected into NIH-3T3 cells. Genomic DNA was amplified with Taq Roche DNA polymerase (Sigma-Aldrich, Zwijndrecht, The Netherlands) using primers against the modified locus and the top 4 potential gene-coding OT (see Section II in the Online Data Supplement for a list of primers). The presence of indels formation was determined using a T7 endonuclease 1 (T7E1) assay, according to manufacturer's instructions (New England Biolabs, Bioké, Leiden, The Netherlands).

AAV9 DNA Vectors

The sgRNAs that appeared the most efficient at inducing DNA strand breaks by in vitro T7E1 assay were cloned into an AAV vector with an expression cassette for Renilla luciferase and the sgRNA backbone—AAV:ITR-U6-sgRNA(backbone)-pEFS-Rluc-2A-Cre-WPRE-hGHpA-ITR was a gift from Feng Zhang (Addgene plasmid no. 60226),[11] which was modified to exclude Cre.

AAV9 Production

Recombinant AAV vectors used in this study were generated by the AAV Vector Unit at ICGEB Trieste (http://www.icgeb.org/avu-core-facility.html) as described previously.[22]

Injection of AAV Vectors Into Neonatal and Adult Mice

Neonatal mice were genotyped at postnatal day 3 (P3) using the Phire Animal Tissue Direct PCR Kit (Fisher Scientific) according to manufacturer's instructions. At P3 or P10, heterozygous (*Myh6*$^{Cas9+/-}$) or homozygous (*Myh6*$^{Cas9+/+}$) *Myh6*^{Cas9} mice or their littermate controls (*Myh6*-Cre negative) were injected with AAV9-sgRNA at either a dose of 5×10^{11} (low dose), 1×10^{12} (medium dose), or 2.5×10^{12} (high dose) viral genomes per animal by intraperitoneal injection. For dual sgRNA delivery, a medium dose was used (this was the maximum dose that could be achieved with the viral titer obtained).

Adult mice (8 weeks) were anesthetized with a low dose mixture of ketamine (60 mg/kg) and xylazine (7 mg/kg) by intraperitoneal injection and intubated with a tracheal tube connected to a ventilator. Mice were supplemented and maintained under anesthesia with 1.5% isoflurane. A surgical plane of anesthesia was confirmed by a lack of a pain reflex. The free wall of the left ventricle was injected with a high dose of AAV9-sg*Sav1* in 2 locations (total volume per injection was 6 µL). The muscle and rib cage were closed with 5-0 silk suture, and analgesia (buprenorphine, 0.05–0.1 mg/kg) were given immediately after surgery and as necessary.

Next-Generation Sequencing and Indel Analysis

For sequencing analysis of indels, we prepared cardiac genomic DNA libraries using customized barcoding methods as described by Junker et al.[23]

Statistics

Data were plotted and analyzed using GraphPad Prism. Data were expressed as mean±SEM. Data were analyzed using a Student *t* test. $P<0.05$ was considered statistically significant.

Results

Generation and Characterization of Cardiomyocyte-Specific Cas9 Mice

The ability to express Cas9 within specific tissues together with the relative ease to deliver sgRNAs postnatally represents an attractive tool to study gene functions in vivo. To investigate the feasibility of CRISPR/Cas9 as a cardiac postnatal gene-editing tool in vivo, we generated mice that express Cas9 in a cardiac-restricted fashion using 2 different approaches. Mice expressing Cre recombinase after the *Myh6* promoter were crossed with homozygous R26-loxP-STOP-loxP-3xFLAG-Cas9-eGFP mouse to generate cardiomyocyte-specific Cas9 mice (*Myh6*^{Cas9} mice; Figure 1A), which concurrently labels all Cas9 cardiomyocytes with eGFP (enhanced green fluorescent protein). In parallel, we generated transgenic mice expressing 3xFLAG and *Streptococcus pyogenes* Cas9 under the control of the *Myh6* promoter. This construct was injected into zygotes to generate cardiomyocyte-specific Cas9 transgenic mice (Online Figure IA). The resulting progenies of both Cas9-expressing mouse models were born at a Mendelian frequency and appeared viable, healthy, and fertile. Relative Cas9 expression in these 2 mouse models was determined by Western blotting against FLAG (Online Figure IB and IC), which showed higher expression of Cas9 in the *Myh6*^{Cas9} mice compared with the transgenic Cas9 mice. We, therefore, decided to use these mice for all subsequent experiments. Whole mount imaging confirmed eGFP (Cas9) expression in the heart of *Myh6*^{Cas9} mice and not in control mice (Figure 1B). We did not detect eGFP expression by stereomicroscope imaging in the liver, lung, kidney, and spleen (data not shown). Confocal imaging confirmed cardiomyocyte-specific expression of Cas9 by costaining with α actinin 2 (Figure 1C). Cardiac-restricted Cas9 expression was confirmed by Western blotting against FLAG and eGFP (Figure 1D). Cas9 was tagged with nuclear localization signals to promote its import into the nucleus, and we confirmed the expression of Cas9 within the nucleus by FLAG immunoblotting, which is fused to Cas9 (Figure 1E). Importantly, the expression of Cas9 in cardiomyocytes did not affect cardiac function and structure up to adulthood as evaluated by morphological and echocardiographic analysis, respectively (Figure 1F–1J). In addition, no changes in gene expression of known cardiac stress markers were detected (Figure 1K).

Design and In Vitro Testing of sgRNAs

To investigate whether our Cas9-expressing mice could be used to perform efficient gene editing in vivo, as a proof-of-concept, we selected 2 important cardiac genes that have previously been studied in knockout mice: T-box 20 (*Tbx20*) and salvador 1 (*Sav1*). *Tbx20* is a cardiac transcription factor critical for both cardiogenesis and cardiac function. Disruption of *Tbx20* in adult mice results in severe dilated cardiomyopathy, arrhythmias, and death as early as 5 days postgenetic ablation.[24] *Sav1* is an integral regulator of the Hippo pathway, which is an evolutionary conserved kinase cascade that serves as a master regulator of development, organ size, and regeneration. Several studies indicate that *Sav1* acts as an endogenous repressor of cardiomyocyte proliferation by promoting the phosphorylation of yes-associated protein, thereby limiting cardiac regeneration.[25,26]

To edit *Sav1* and *Tbx20*, we designed sgRNAs against the genes using the CRISPR design tool (http://crispr.mit.edu/), which systematically screens for OT effects.[20] The 20-nucleotide sequences were designed to precede a CRISPR type II–specific protospacer-adjacent motif sequence 5′–NGG. Four sgRNAs (targeting exon 1 for *Tbx20* and exon 3 for *Sav1*; based on previous strategies to generate knockout mice[27,28]) were designed and cloned into a Cas9-expressing vector and transfected into NIH-3T3 cells (Figure 2A). Based on the

Downloaded from http://circres.ahajournals.org/ by guest on February 6, 2018

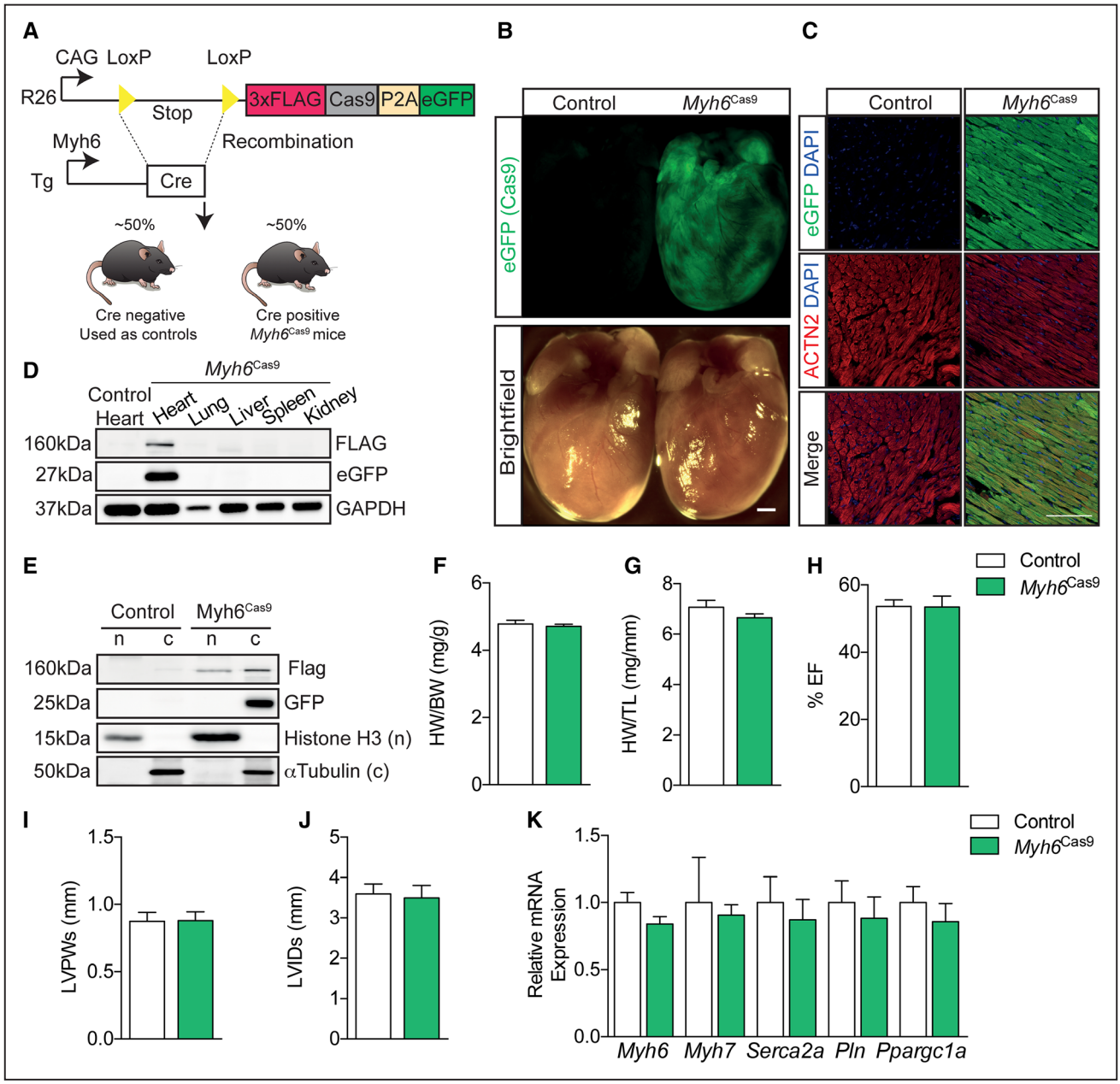

Figure 1. Generation and characterization of a cardiomyocyte-specific Cas9 (CRISPR-associated protein 9)–expressing mouse. **A**, Strategy for the generation of Myh6^{Cas9} mice. **B**, Fluorescence (eGFP [enhanced green fluorescent protein]; Cas9) and brightfield stereomicroscope images of whole hearts isolated from control and Myh6^{Cas9} mice. Scale bar is 1 mm. **C**, Immunofluorescence expression of eGFP (Cas9), sarcomeric α actinin (ACTN2; cardiomyocytes), and 4′,6-diamidino-2-phenylindole in fixed heart histological sections. Scale bar is 100 μm. **D**, Western blot validation of cardiac-specific expression of FLAG and eGFP in Myh6^{Cas9} mice. GAPDH was used as a loading control. **E**, Western blot showing nuclear (n) and cytoplasmic (c) localization of Cas9 by FLAG expression. Heart weight/body weight ratio (HW/BW). **F** and **G**, HW/tibia length (HW/TL) ratio. Echocardiographic analysis of cardiac function and structure by (**H**) % ejection fraction (EF), (**I**) left ventricular posterior wall thickness at systole (LVPWs), and (**J**) LV internal diameter at s (LVIDs). **K**, mRNA analysis of cardiac stress markers by quantitative reverse transcription polymerase chain reaction. Data were normalized to *Gapdh*. Data are represented as the mean±SEM. n=4 to 8 mice per group. Myh6 indicates myosin heavy chain 6; *Pln*, phospholambam; *Ppargc1a*, peroxisome proliferator-activated receptor γ coactivator 1-α; *Serca2a*, sarco/endoplasmic reticulum Ca^{2+}-ATPase; and tg, transgenic.

efficiency of the sgRNA-induced DNA DSBs, as assessed by T7E1 analysis in puromycin selected (Cas9 and sgRNA transfected) cells, we selected guide 1 and guide 2 to target the *Tbx20* and *Sav1* locus, respectively (Figure 2B and 2C). The efficiency was determined by calculating the percentage of indels by band intensity quantification (see Section I in the Online Data Supplement). Guides were designed to minimize potential OT effects in other sites within the genome. To confirm the fidelity of our sgRNA design, we performed T7E1 assays on amplified DNA from the top 4 predicted OT protein-coding genes for each sgRNA, and no OT indels were observed (Figure 2D and 2E). The sequence of the selected sgRNAs for each target and its genomic target location are shown in Figure 2F. We next determined the effect of DNA

Downloaded from http://circres.ahajournals.org/ by guest on February 6, 2018

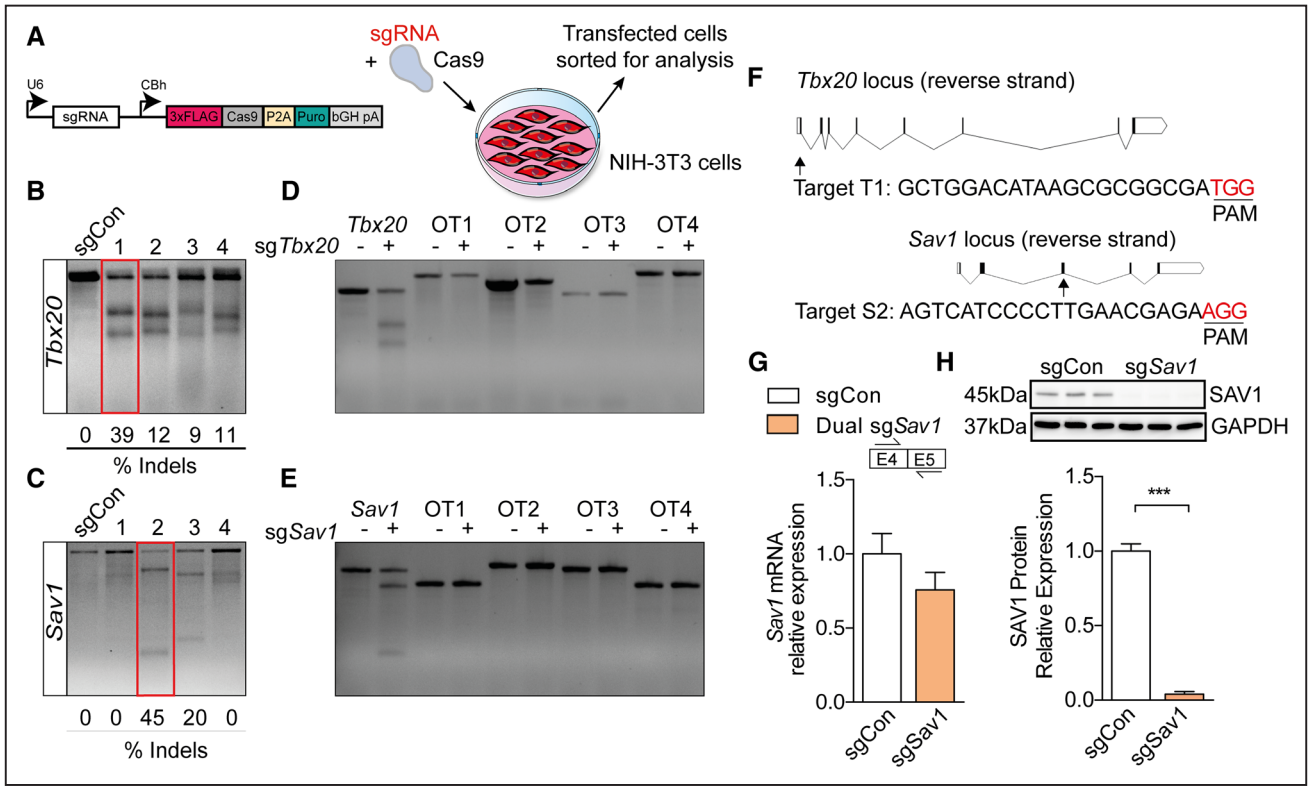

Figure 2. Short guide RNA (sgRNA) generation and in vitro gene editing using CRISPR/Cas9 (clustered regularly interspaced palindromic repeats/CRISPR-associated protein 9). **A**, Schematic of the sgRNA-Cas9 vector and in vitro experiment in NIH-3T3 cells. T7 endonuclease 1 (T7E1) analysis on target site of polymerase chain reaction (PCR)–amplified genomic DNA from sorted NIH-3T3 cells transfected with either a control sgRNA (sgCon) or sgRNAs designed to target (**B**) T-box 20 (*Tbx20*) or (**C**) salvador 1 (*Sav1*). Red box indicates the selected sgRNA. **D** and **E**, T7E1 of PCR-amplified genomic DNA from sorted NIH-3T3 for the top 4 potential off-target (OT) DNA cleavage sites in gene-coding regions for the selected sgRNA for (**D**) *Tbx20* and (**E**) *Sav1*. **F**, Targeted genomic locus and sequence of selected sgRNAs. Effect of sg*Sav1*-mediated gene disruption in sorted cells on (**G**) mRNA expression and (**H**) protein expression. GAPDH was used as the loading control. Data are represented as the mean±SEM. n=3 replicates per group.

disruption in NIH-3T3 cells on subsequent transcription and translation of the target genes. Because we could not reliably detect *Tbx20* transcript or protein expression in NIH-3T3 cells, likely because it is not expressed (data not shown), we determined the effect of sgRNA-mediated disruption on *Sav1*. This resulted in a reduction in *Sav1* transcription and translation as assessed by quantitative reverse transcription PCR analysis (Figure 2G) and Western blotting (Figure 2H) for sg*Sav1* compared with sgControl samples.

In Vivo Genome Editing of the Heart Using Systemic Delivery of sgRNAs With AAV9

Having identified functional sgRNAs, we incorporated the in vitro selected sgRNAs into a U6-driven AAV backbone and selected the cardiotropic AAV9 as the delivery vector (Figure 3A). Mice were injected intraperitoneal with a single dose (5×10^{11} vg/mouse) of AAV9-sgRNA at P3 and were analyzed 2 weeks later at P17 (Figure 3A). Administration of AAV9 by intraperitoneal injection in neonatal mice has previously been shown to mediate robust cardiac gene expression.[29,30] Quantitative reverse transcription PCR analysis of sgRNA expression showed that the sgRNA is indeed expressed and that its expression is stabilized specifically in the heart by Cas9 (Online Figure IIA). We confirmed that the increase in sgRNA expression in Cas9-expressing mice was not related to an increased viral dose by assessing luciferase mRNA expression (encoded by the construct; Online Figure IIB). As an indication of overall health, body weights were monitored daily, and this was not affected by the sgRNA-mediated editing (data not shown). Furthermore, we observed no effect on cardiac size as determined by the heart weight/tibia length ratio (Online Figure IIC). T7E1 analysis of DNA isolated from whole hearts demonstrated DNA disruption at the targeted loci for *Tbx20* and *Sav1* in $Myh6^{Cas9}$ mice while the sgRNAs had no effect in control littermates (Figure 3B and 3C, respectively). Importantly, no DNA DSBs were observed in the kidney, lung, liver, or spleen of $Myh6^{Cas9}$ mice confirming the cardiac-restricted Cas9 expression (Online Figure IIF and IIG). A reduction in mRNA expression was observed for both targets (Figure 3D). We confirmed this reduction using 3 additional primer pairs (Online Figure IID and IIE). Furthermore, no difference in *Tbx20* or *Sav1* mRNA expression was detected in uninjected control and $Myh6^{Cas9}$ mice, confirming a sgRNA mediated effect (data not shown). However, despite a reduction in mRNA transcript levels, this only translated into a small reduction in protein expression for *Tbx20* and no effect on *Sav1* (Figure 3E–3G). Furthermore, we could not detect a transcriptional effect on known downstream targets (Online Figure IIH and III). To further evaluate the gene-editing effects within cardiomyocytes, we performed immunohistochemistry analysis

Downloaded from http://circres.ahajournals.org/ by guest on February 6, 2018

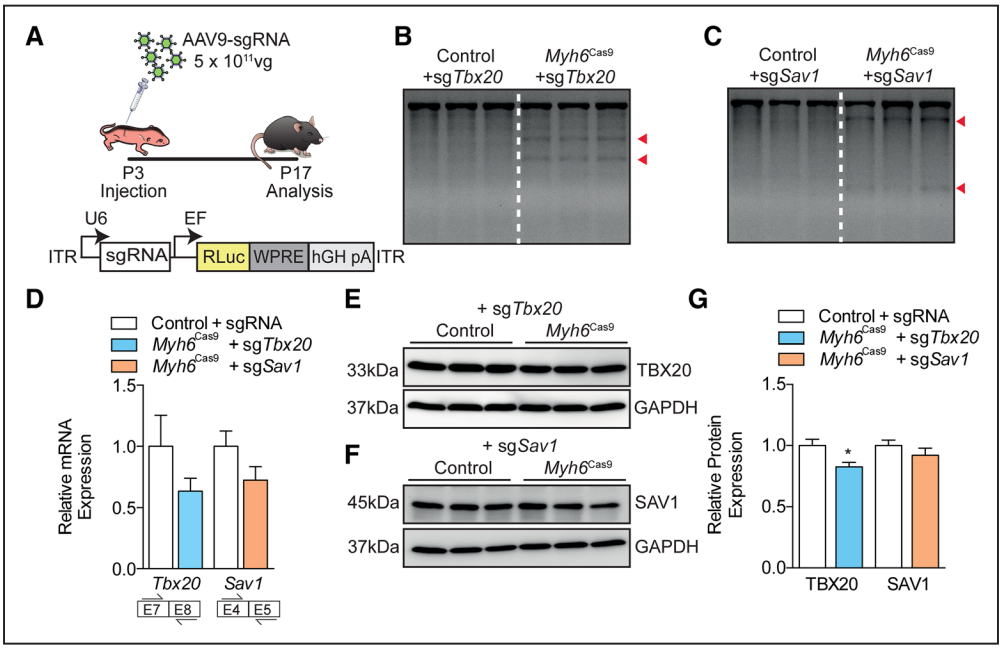

Figure 3. In vivo genome editing in the heart of a cardiomyocyte-specific Cas9 (CRISPR-associated protein 9) mouse. **A**, Schematic of study outline and short guide RNA (sgRNA) vector incorporated into adeno-associated virus serotype 9 (AAV9). **B** and **C**, T7 endonuclease 1 (T7E1) analysis on target site of polymerase chain reaction (PCR)–amplified genomic DNA from isolated hearts. Red arrowheads indicate cut bands by T7E1. **D**, Cardiac T-box 20 (*Tbx20*) and salvador 1 (*Sav1*) mRNA analysis by quantitative reverse transcription PCR using primer pairs as indicated. **E**–**G**, Representative Western blot and quantification for cardiac TBX20 and SAV1 expression. GAPDH was used as the loading control. Data are represented as the mean±SEM. **P*<0.05, n=5 to 8 mice per group.

for TBX20, as its nuclear localization allows for quantification of TBX20-positive and -negative cardiomyocytes. TBX20 expression was found to be decreased in *Tbx20*-edited mice (Online Figure IIJ and IIK). Taken together, these results suggest that there is inefficient gene editing in these mice.

To evaluate whether the viral titer (and therefore the levels of sgRNA) or the exposure time to the sgRNA could improve the targeting efficiency of Cas9, we used the same viral backbone and injected mice with either a low (5×10^{11} vg/mouse) or high (2.5×10^{12} vg/mouse) dose of AAV9-sg*Tbx20* (Online Figure IIIA). Mice were analyzed 4 weeks later (Online Figure IIIA), and successful DNA DSBs were confirmed by T7E1 analysis for both viral doses (Online Figure IIIB and IIIC). Here, we observed that although the low dose of virus did not affect gene expression, the high dose of sgRNA resulted in a downregulation of mRNA transcripts. (Online Figure IIID). However, for both the low and high doses, we again could not detect an effect on protein expression (Online Figure IIIE–IIIG).

Given that a higher viral dose mediated a greater effect on gene disruption, we selected this dose for subsequent experiments. We next evaluated whether a longer exposure period would improve targeting efficiency rates. To do so, we injected mice with either AAV9-sg*Tbx20* or -sg*Sav1* and harvested tissue 8 weeks later (Online Figure IVA). T7E1 analysis of whole heart homogenates determined successful DNA cleavage in *Myh6*^{Cas9} mice injected with AAV9-sg*Tbx20* and sg*Sav1* (Online Figure IVB and IVC). No effect on mRNA transcript levels was observed in sg*Tbx20*-edited mice, yet an ≈50% reduction in mRNA transcripts was observed in the sg*Sav1*-edited mice (Online Figure IVD). This suggests a loss of edited cells over time in the sg*Tbx20*-treated mice, similar to what was observed in the mice treated with a low dose of virus for 4 weeks.

Because a longer duration and a higher viral dose failed to mediate a more robust target disruption, we next asked whether increased Cas9 expression could improve targeting efficiency. To do so, we generated homozygous cardiomyocyte-specific Cas9 mice and showed that eGFP (Cas9) expression was increased compared with heterozygous cardiomyocyte-specific Cas9 mice (Online Figure VA and VB). Homozygous Cas9 mice and their Cre- littermate controls were injected with either AAV9-sg*Tbx20* or -sg*Sav1* and analyzed 2 weeks later (Online Figure VC). T7E1 analysis of whole heart homogenates showed successful gene disruption (Online Figure VD and VE) and a subsequent reduction in mRNA expression in the homozygous Myh6^{Cas9} mice (Online Figure VF). However, no effect on protein expression was detected (Online Figure VG–VI), suggesting that increased Cas9 expression did not improve the targeting efficiency.

In Vivo Genome Editing of the Heart by Local Delivery of sgRNAs Using AAV9

Because our results indicated that the systemic AAV9-sgRNA delivery failed to mediate efficient cardiac gene editing, we next questioned whether the local delivery of sgRNAs could improve targeting efficiency rates. We injected adult mice (8 weeks old) with AAV9-sg*Sav1* directly into the left ventricular myocardial wall and analyzed mice 2 weeks later (Online Figure VIA). We attempted to specifically isolate the AAV9-sg*Sav1*–injected region of the myocardial wall. By T7E1 analysis, we were able to detect some DNA disruption (Online Figure VIB); however, no effect was apparent on mRNA

Downloaded from http://circres.ahajournals.org/ by guest on February 6, 2018

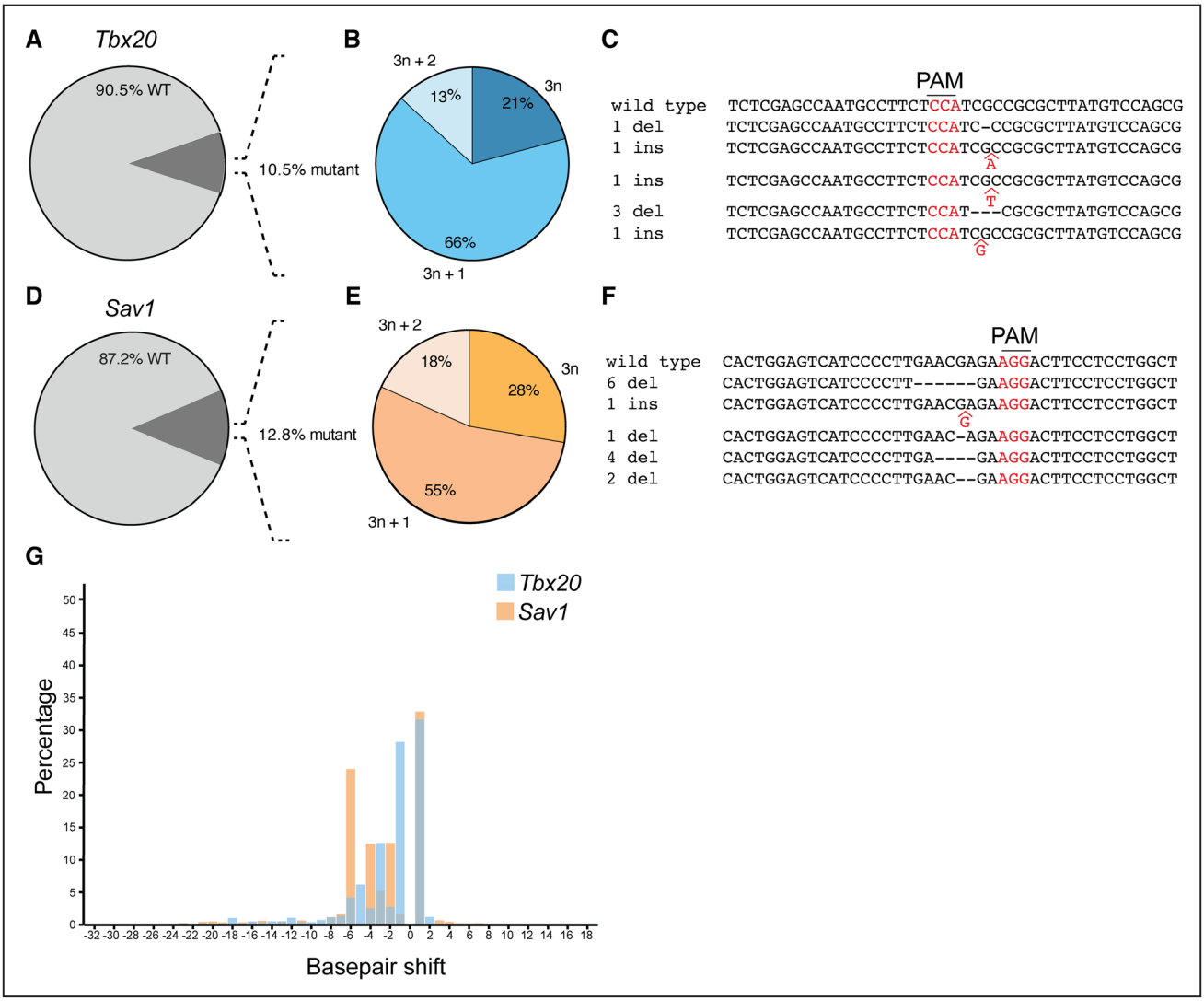

Figure 4. In-depth indel analysis of in vivo T-box 20 (*Tbx20*) and salvador 1 (*Sav1*) cardioediting by DNA sequencing. Deep sequencing analysis of the *Tbx20* and *Sav1* locus of hearts isolated at P17 from mice injected with an short guide RNA (sgRNA) at P3 (from Figure 3A). **A**, Percentage of mutant reads in adeno-associated virus serotype 9 (AAV9)-sg*Tbx20*–injected Myh6^{Cas9} mice and (**B**) the corresponding indel analysis and (**C**) the most abundant sequencing reads. **D**, Percentage of mutant reads in AAV9-sg*Sav1*–injected Myh6^{Cas9} mice and (**E**) the corresponding indel analysis and (**F**) the most abundant sequencing reads. **G**, Size distribution of indels found at each sgRNA targeting site. Data are the average of 4 mice. Myh6 indicates myosin heavy chain 6; and WT, wild type.

expression levels (Online Figure VIC), showing that local delivery of sgRNAs did not improve the editing capacity.

In-Depth Indel Analysis Using DNA Sequencing Demonstrates Target-Dependent Indels

Because our results demonstrated cardiac editing in all our studies by T7E1 analysis, the absence of effect on protein expression, downstream gene targets, and the expected cardiac phenotype likely indicates a mosaic pattern of gene disruption. To precisely determine the level of cardioediting, we performed DNA sequencing of the *Tbx20* and *Sav1* locus on the hearts isolated from *Myh6*^{Cas9} (see Section I in the Online Data Supplement for details of DNA sequencing set-up and analysis). In control mice, the detected % of mutated DNA was 0.1% to 0.2%. In AAV9-sg*Tbx20*–injected mice, we detected ≈10.5% of mutated reads (Figure 4A; Online Figure VIIA), of which ≈21% were in-frame (3n) mutations (Figure 4B and 4C; Online Figure VIIB and VIIC). However, the majority of the mutations were out-of-frame (≈79%; 3n+2 or 3n+1). In AAV9-sg*Sav1*–injected mice, we detected ≈12.8% of mutated reads (Figure 4D; Online Figure VII7D), of which ≈28% were in-frame and again the majority (≈72%) were out-of-frame mutations (Figure 4E and 4F; Online Figure VIIE and VIIF). Of interest, we observed target-specific indels, which were detected in all mice analyzed (Figure 4G; Online Figure VIIG).

Cardiomyocytes contribute to ≈30% of the total cells that make up the myocardial wall, yet because of their large structure, they contribute to ≈70% of the myocardial volume.[31] Thus, because Cas9 is only active in cardiomyocytes, the percentage of mutated DNA is diluted by noncardiomyocytes by approximately two thirds, and we therefore estimate that the percentage of edited cells is ≈31.5% for *Tbx20* and ≈38.4% for *Sav1*.

Downloaded from http://circres.ahajournals.org/ by guest on February 6, 2018

Downloaded from http://circres.ahajournals.org/ by guest on February 6, 2018

In Vivo Genome Editing of *Myh6* Using Systemic Delivery of sgRNAS With AAV9 Results in a Severe Dilated Cardiomyopathy

Although our results suggested that using a single sgRNA delivered by AAV9 is inefficient to mediate robust gene editing to study gene knockout, a recent study reported efficient postnatal genome editing in vivo in the heart using CRISPR/Cas9.[13] In this study, the disruption of exon 3 (the first coding exon) of *Myh6* using AAV9-delivered sgRNAs in *Myh6* Cas9 transgenic mice resulted in a severe dilated cardiomyopathy with compromised cardiac contractility.[13] These results recapitulated the results reported in *Myh6* heterozygous and homozygous knockout mice.[32] To determine whether our lack of a gene-editing effect was related to the gene target, mouse model, or viral dose, we performed a side-by-side comparison with the virus used in this study (courtesy of Prof Eric Olson) to disrupt *Myh6*. We injected our mice with sg*Myh6* and sg*Tbx20* at 1×10^{12} viral genomes at P10 and analyzed mice 5 to 6 weeks post-injection, an experimental design identical to the published study (Figure 5A). As expected, AAV9-sg*Myh6*–injected mice developed a severe cardiac phenotype (Figure 5B–5H) with a reduced ejection fraction (Figure 5C), left ventricular dilation (Figure 5D–5F), and an increased heart weight/tibia length ratio (Figure 5G and 5H). In the *Tbx20*-edited mice, a small, yet significant increase in ejection fraction (Figure 5C), as well as a reduction in the left ventricular internal diameter (Figure 5D), was measured in the absence of changes in cardiac morphology or the heart weight/tibia length ratio (Figure 5G and 5H).

Because the sgRNAs were delivered using different vector backbones, we determined sgRNA expression in the injected mice by quantitative reverse transcription PCR. We found that sgRNA expression levels were similar in all control mice injected with either virus and that its expression was increased by Cas9, which was more evident in sg*Tbx20*-injected mice (Figure 5I). T7E1 analysis of the targeted locus-amplified genomic DNA confirmed cardiac editing for both genes (Figure 5J and 5K), which was accompanied by a reduction in mRNA expression, to a similar degree in both sgRNA-injected mice (Figure 5L). Different primers were used to detect *Tbx20* here compared with previously to better reflect the primers used for detection of *Myh6* (see Section I in the Online Data Supplement for details). Western blotting for TBX20 and MYH6 (with an antibody that does not cross-react with MYH7) showed a significant reduction in protein expression, which was more apparent in *Myh6*-edited mice (Figure 5M–5O). Furthermore, we were further able to validate the increased expression of the cardiac stress markers *Myh7*, *Nppa*, and *Nppb* in the *Myh6*-edited mice (Figure 5P), which was also observed previously in *Myh6*-edited[13] and heterozygous *Myh6* knockout mice.[32]

To determine the percentage of edited DNA in these mice, we performed in-depth indel analysis by DNA sequencing of cardiac samples from *Tbx20*- and *Myh6*-edited mice. This showed that ≈22% and ≈4% of the target locus was mutated for AAV9-sg*Tbx20* and -sg*Myh6*, respectively (Figure 6; Online Figure VIII). In our *Tbx20*-edited mice, from the 4 mice analyzed, 1 mouse had a much higher percentage of mutant reads (≈45%), which increased the average number of mutant reads. In the other 3 mice, mutant reads constituted ≈11% to 15% of the total reads (Figure 6A; Online Figure VIIIA). The frequency and type of mutations observed in the *Tbx20*-edited mice were similar to our previous data in mice treated at P3 and analyzed 2 weeks later (Figure 4D–4F; Online Figure VIIID–VIIIF), suggesting that age and incubation time does not affect the type and frequency of indels introduced. The majority of the mutations (≈86%) were out-of-frame mutations (Figure 6B and 6C; Online Figure VIIIB and VIIIC). In the *Myh6*-edited mice, we detected ≈3.8% mutated reads, of which the majority (≈91%) were out-of-frame mutations (Figure 6E and 6F; Online Figure VIIIE and VIIIF). Thus, for both targets, these mutations are likely to disrupt endogenous gene function in the cells that are edited. As observed in our previous data (Figure 4G; Online Figure VIIG), each sgRNA mediates target-specific indels (Figure 6G; Online Figure VIIIG). Finally, in control mice, the detected % of mutated DNA was 0.1% to 1.1%.

Taken together, these data show that despite low mutation frequencies, in particular in *Myh6*-edited mice, and subsequent downregulation in transcription for *Tbx20*- and *Myh6*-edited mice, only *Myh6*-edited mice develop a cardiomyopathy. Strikingly, the degree of *Myh6* targeting and mRNA downregulation correlated with the severity of the cardiac phenotype, fold change sgRNA, and cardiac stress marker expression (Table).

AAV9 Is an Efficient Tool to Deliver sgRNAs by Systemic Injection

Our results show that a higher viral dose resulted in increased Cas9-mediated DNA cleavage (see Online Figure III comparing low dose with high dose). To determine whether the AAV9 delivery of the sgRNA was the limiting factor, we used the sgRNA-ZsGreen construct to trace sgRNA delivery in the heart (Online Figure IXA and IXB). We determined that both a low and high viral dose targets a substantial number of cardiomyocytes (≈60%–≈70%) although with varied expression within cells (Online Figure IXA and IXB). Because of the difference in ZsGreen expression within cells between the doses, it was not possible to image them with the same settings—for the high dose, the fluorescence intensity was reduced for both stereomicroscopy and confocal imaging. Thus, cells targeted with the high viral dose expressed more ZsGreen (sgRNA). Overall, this suggests that a sufficient number of cardiomyocytes are targeted and that increasing the viral titer will increase sgRNA expression within cells.

Chromatin Accessibility of Target Genes

Heterochromatic regions within the genome are less accessible to Cas9, thus reducing its efficiency.[33] mRNA transcript analysis of *Sav1*, *Myh6*, and *Tbx20* suggested that they are expressed at high levels within cardiac tissue. However, to rule out the possibility that Cas9 efficiency is reduced at our targeted sites because of heterochromatic regions, we determined chromatin accessibility in our sgRNA target sites in publicly available Chip-seq databases for neonatal mouse hearts.[34] All gene loci containing the sgRNA recognition site displayed features of open chromatin, including the active

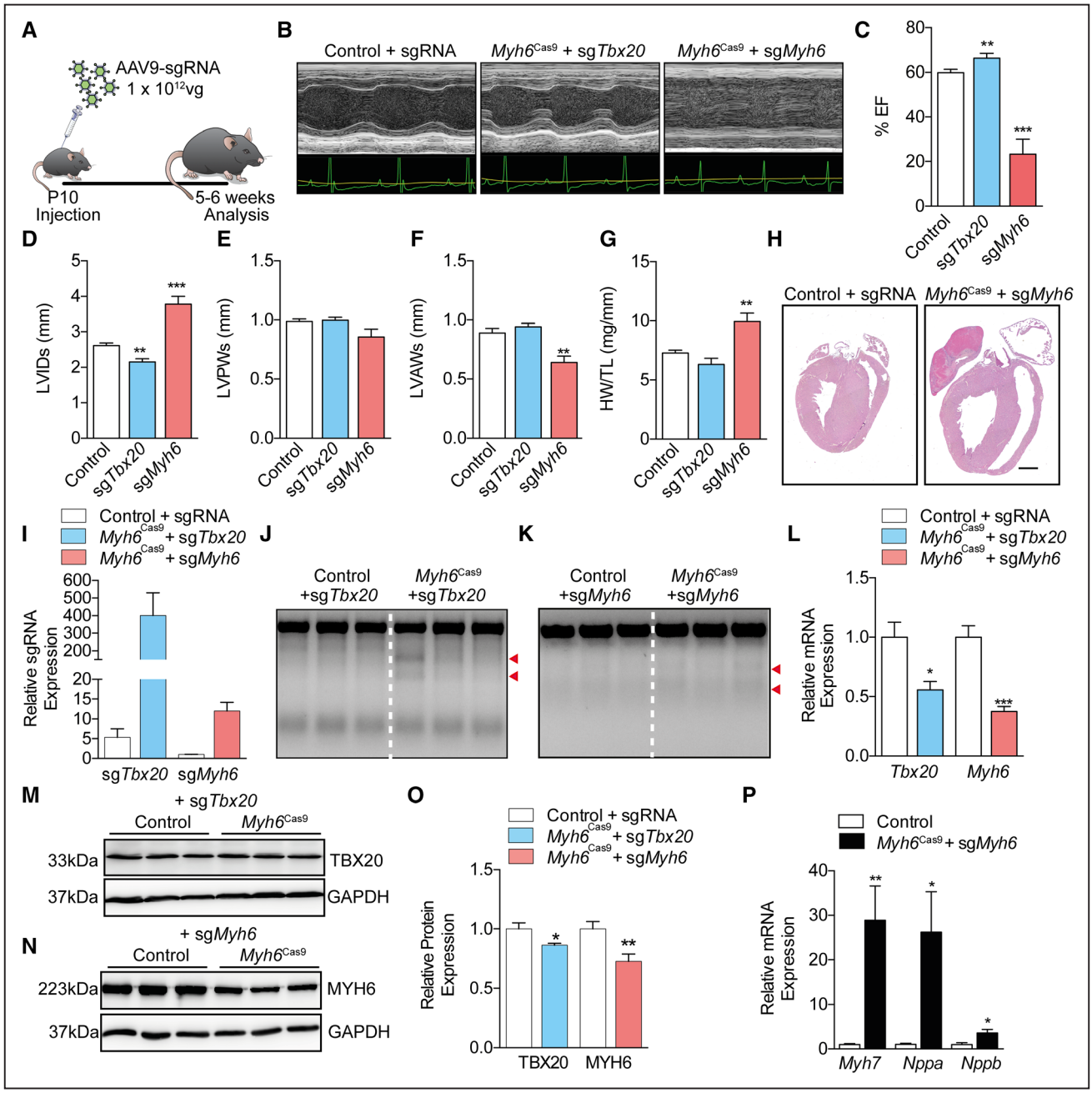

Figure 5. In vivo cardioediting with CRISPR/Cas9 (clustered regularly interspaced palindromic repeats/CRISPR-associated protein 9) is target dependent. A, Schematic of study outline. **B**, Representative echocardiographic recordings shown in M-mode of control and Myh6^{Cas9} mice injected with either adeno-associated virus serotype 9 (AAV9)-sg*Tbx20* or -sg*Myh6*. Echocardiographic analysis of cardiac function and structure by (**C**) % ejection fraction (EF), (**D**) left ventricular (LV) internal diameter at systole (LVIDs), (**E**) LV posterior wall thickness (LVPW), and (**F**) LV anterior wall (LVAW) at systole. **G**, Heart weight/tibia length ratio (HW/TL). **H**, Representative hematoxylin and eosin–stained 4-chamber view of heart from control and Myh6^{Cas9} mice injected with sg*Myh6*. Scale bar is 1 mm. **I**, Short guide RNA (sgRNA) expression in the heart of sg*Tbx20*- and sg*Myh6*-treated mice. Control+sg*Tbx20*, n=3; Myh6^{Cas9}+sg*Tbx20*, n=5; control+sgMyh6, n=4; Myh6^{Cas9}+sg*Myh6* n=8. **J** and **K**, T7 endonuclease 1 (T7E1) analysis on target site of polymerase chain reaction (PCR)–amplified genomic DNA from isolated hearts. Red arrowheads indicate cut bands by T7E1. **L**, Cardiac *Tbx20* and *Myh6* mRNA analysis by quantitative reverse transcription (qRT)-PCR. **M**–**O**, Representative Western blot and quantification for cardiac TBX20 (**M**) and MYH6 (**N**) expression. GAPDH was used as the loading control. **P**, Expression of cardiac stress markers, myosin heavy chain 7 (*Myh7*), natriuretic peptide type A/B (*Nppa/b*) mRNA analysis by qRT-PCR in *Myh6*-edited mice. Data are represented as the mean±SEM. **P*<0.05, ***P*<0.01; ****P*<0.001, n=5 to 9 mice per group, unless indicated otherwise. Myh6 indicates myosin heavy chain 6; and *Tbx20*, T-box 20.

enhancer mark H3k27Ac and DNase-Seq hotspots (regions that are more susceptible to DNase activity because of less nucleosomes), confirming that the target sites should all be accessible for Cas9 in the heart (Online Figure X).

Dual sgRNA Strategy to Mediate Precise Genome Editing

Because our results highlighted inefficient targeting using a single sgRNA, we next sought to determine whether the

Downloaded from http://circres.ahajournals.org/ by guest on February 6, 2018

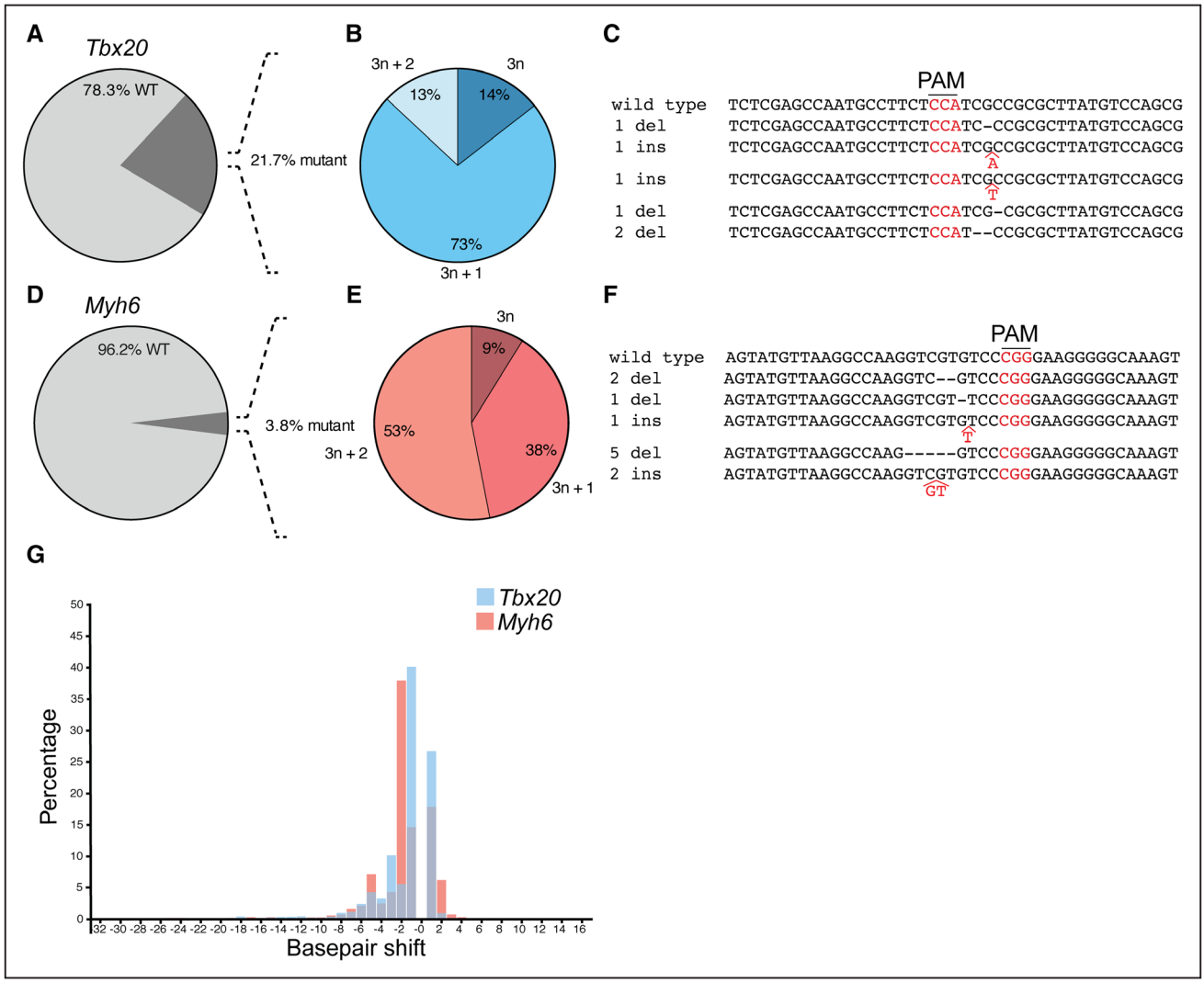

Figure 6. In-depth indel analysis of in vivo T-box 20 (*Tbx20*) and myosin heavy chain 6 (*Myh6*) cardioediting by DNA sequencing. Deep sequencing analysis of the *Tbx20* and *Myh6* locus of hearts isolated at 5 to 6 wk of age from mice injected with a short guide RNA (sgRNA) at P10 (from Figure 5A). **A**, Percentage of mutant reads in adeno-associated virus serotype 9 (AAV9)-sg*Tbx20*–injected Myh6^{Cas9} mice and (**B**) the corresponding indel analysis and (**C**) the most abundant sequencing reads. **D**, Percentage of mutant reads in AAV9-sg*Myh6*–injected Myh6^{Cas9} mice and (**E**) the corresponding indel analysis and (**F**) the most abundant sequencing reads. **G**, Size distribution of indels found at each sgRNA targeting site. Data are the average of 3 to 4 mice. WT indicates wild type.

simultaneous use of a dual sgRNA could facilitate enhanced efficiencies. We designed 2 sgRNAs to remove exon 3 of *Sav1* containing the essential WW45 binding domain—the same approach that was used to generate *Sav1* knockout mice.[27] Based on the predicted sgRNA cutting sites, we determined that the selected sgRNAs would remove exon 3 and introduce a stop codon in the transcript read in exon 4 (Figure 7A). Using 2 separate vectors, we tested the functionality of this approach in NIH-3T3 cells (Figure 7B). PCR analysis revealed a efficient deletion of the exon by the 275 bp expected reduction in DNA size (Figure 7C), and this was confirmed by Sanger sequencing (Figure 7D). Although we could not detect any changes on mRNA expression, a robust downregulation in protein expression was detected (Figure 7E and 7F).

Having demonstrated successful gene editing in vitro, we generated a dual sgRNA AAV9 virus to deliver the sgRNAs in vivo. Mice were injected at P3 with 1×10^{12} viral genomes and analyzed 2 weeks later, as with our previous studies using a single sgRNA in heterozygous and homozygous mice (Figure 7G). PCR analysis revealed exon deletion in *Myh6*^{Cas9} mice injected with the dual sgRNA (Figure 7H). Dual sgSav1-treated mice had a modest enlargement in their hearts as assessed by the heart weight/tibia length ratio (Figure 7I), suggesting the expected increase in cardiac proliferation as observed in Sav1 knockout hearts.[26] We validated the increase in cardiac proliferation by quantitative reverse transcription PCR for cyclin D1 and *Ki67* (Figure 7J). Furthermore, we also found an increase in the hypertrophic markers, Nppa and Nppb (Figure 7J). Although we could not detect a consistent reduction in SAV1 mRNA and protein expression (Figure 7K through 7M), we observed an upregulation of downstream SAV1 targets (Figure 7N), which we had previously (Online Figure IIH) failed to detect. In a separate experiment, we also tried injecting 2 separate AAV9-sgRNA vectors, which resulted in exon deletion, but the results were less effective with no

Downloaded from http://circres.ahajournals.org/ by guest on February 6, 2018

Table. Correlation of CRISPR/Cas9-Mediated Disruption of *Myh6* With Cardiac Phenotype and Gene Expression

No.	% Indels	Relative Myh6	% EF	LVID mm	HW/TL Ratio	Relative sgRNA	Relative *Myh7*	Relative *Nppa*	Relative *Nppb*
1	2.33	0.61	65.59	2.40	8.10	6.28	1.81	2.19	1.75
2	3.33	0.39	43.70	3.34	7.90	10.31	7.91	6.45	2.33
3	N/A	0.36	27.85	3.45	6.74	12.22	18.63	0.84	2.51
4	N/A	0.36	24.76	4.10	9.19	13.21	34.56	52.76	7.76
5	N/A	0.32	6.79	4.43	10.26	15.20	53.32	53.71	3.62
6	N/A	0.30	8.69	4.27	10.53	4.80	52.37	23.28	2.36
7	5.89	0.29	4.09	4.38	11.53	21.98	33.58	44.64	5.00

Mice were ranked based on the mRNA expression of *Myh6*. % indels (mutated DNA) are shown in the mice where it was measured. mRNA data are the relative fold change in mRNA expression relative to control littermate mice. CRISPR/Cas9 indicates clustered regularly interspaced palindromic repeats/CRISPR-associated protein 9; EF, ejection fraction; HW/TL, heart weight/tibia length; indels, insertion deletions; LVID, left ventricular internal diameter; Myh6, myosin heavy chain 6; N/A, not applicable; and sgRNA, short guide RNA.

Downloaded from http://circres.ahajournals.org/ by guest on February 6, 2018

effect on heart weight or Sav1 downstream targets at either 2 or 4 weeks post-injection, highlighting the importance of using a dual sgRNA vector to permit synergistic cutting by Cas9 (data not shown).

Discussion

The discovery that Cas9 can be redirected to mediate highly precise genome editing has demonstrated enormous versatility to study gene function, yet its application to study postnatal cardiomyocyte-specific knockouts remains uncharacterized. Here, we generated cardiomyocyte-specific Cas9 mice and demonstrated that Cas9 expression alone does not affect cardiac function or the expression of cardiac stress markers, which is in line with other studies expressing Cas9 constitutively in the heart.[13] We targeted 3 genes critical for cardiac physiology, *Myh6*, *Tbx20* (critical for cardiac function), and *Sav1* (impedes cardiac regeneration), and despite a similar degree of gene disruption, we only observed a cardiac phenotype in *Myh6*-edited mice. Previous studies have focused on disrupting genes that are critical for cardiomyocyte function, yet our study is the first, to our knowledge, to target a nonlethal gene (*Sav1*). Our results suggest that viral delivery of sgRNAs to the heart introduces mosaic gene disruption, whereby only a subset of cells are edited, presenting important limitations for the current application of AAV9-mediated delivery of sgRNAs for cardioediting. Our data are in concert with what has been recently reported by others in the field.[15] Finally, we show that a dual sgRNA approach is essential to maximize the percentage of effectively edited cells.

Although a broad evaluation of the feasibility of using Cas9 to perform postnatal gene editing of the heart was lacking to generate knockouts, recent studies have shown successful application of the technology in the heart using similar approaches to our experimental design.[13–15] In a study by Xie et al,[14] they generated heterozygous *PRKAG2* mutant mice that developed cardiac hypertrophy, recapitulating the clinical symptoms observed in patients with Wolff–Parkinson–White syndrome. By AAV9-mediated delivery of Cas9 and a single sgRNA directed at disrupting the mutant allele, the authors restored a normal cardiac function in these mice. Here, using DNA sequencing, an indel frequency of 6.5% and 2.6% was measured in mice injected at P4 and P42, respectively, which is comparable with the ≈4% to 15% editing frequency observed in our study (Figures 4 and 6). These results potentially suggest that cardioediting using AAV9 is more permissible in younger mice, perhaps because of the more proliferative state of the cardiomyocytes. This is supported by the fact that we could not detect an effect on mRNA expression in adult mice injected with AAV9-sg*Sav1* directly into the myocardial wall (Online Figure VI). Although disruption of the PRKAG2 mutant allele resulted in less mRNA transcripts, no measurable effect was reported on the protein expression of the target[14] as was shown in our study for *Tbx20* and *Sav1*. In contrast, for *Myh6*, we observed a significant reduction in protein expression.

Here, we demonstrated that disruption of <5% of *Myh6* was sufficient to drive a severe cardiomyopathy (Figures 5 and 6), which is in line with the previous study cardioediting *Myh6*.[13] We speculate that the slightly smaller percentage of edited cells in the *Myh6*-edited mice may be because of apoptosis of the mutated cells although this would have also been expected in the *Tbx20*-edited mice. The fact that a similar disruption of *Tbx20* and *Sav1* (≈10%–15%) failed to reproduce the cardiac phenotype reported in knockout models using a single sgRNA may be a result of the sensitivity of the target gene to small perturbations in gene expression. Both heterozygous and homozygous *Myh6* knockout mice develop a severe cardiomyopathy,[32] highlighting the sensitivity of this gene to genetic alterations. Thus, for the purpose of gene editing to disrupt mutant alleles or where mosaic targeting is sufficient (such as in muscular dystrophy), CRISPR/Cas9 may be a useful tool. However, for the generation of knockout mice or to study unknown cardiac gene functions, the CRISPR/Cas9 system in its current form is less suitable. If the effect on overall cardiac function is not essential or novel genes are being studied, we would recommend the isolation of targeted cells for downstream analysis. Mosaic gene disruption is particularly attractive when studying genes of which disruption rapidly results in the onset of cardiomyopathy because mosaic targeting would allow mechanistic analysis of gene disruption in vivo. This has been recently elegantly shown by Guo et al.[15]

We used AAV9 to specifically target Cas9-expressing cardiomyocytes and showed that ≈60% to 70% were successfully

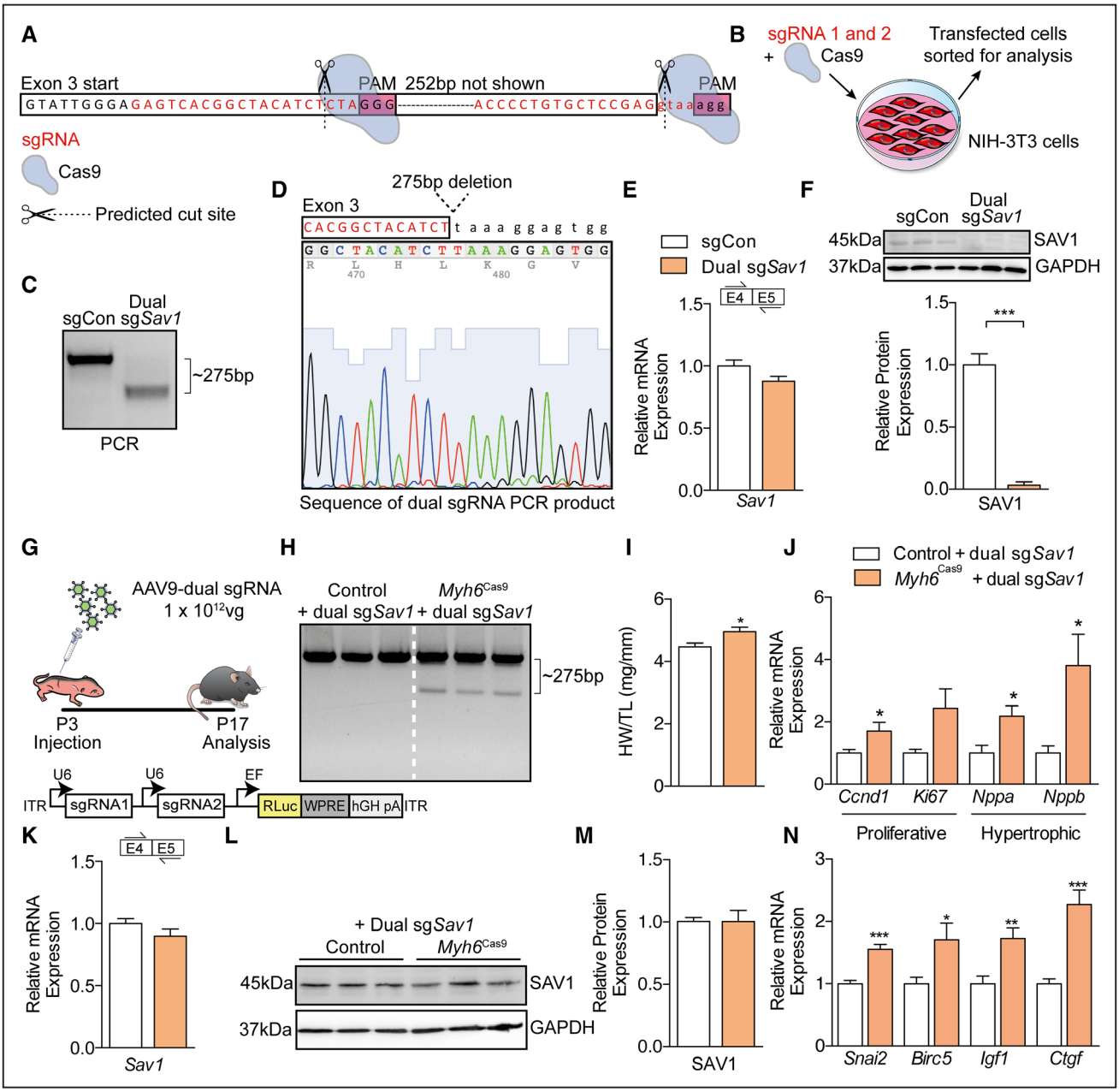

Figure 7. CRISPR/Cas9 (clustered regularly interspaced palindromic repeats/CRISPR-associated protein 9)–mediated cardiac genome editing using a dual short guide RNA (sgRNA) strategy to knockdown salvador 1 (*Sav1*). A, sgRNAs were designed to delete 275 bp from exon 3. **B**, Separate sgRNA-Cas9 plasmids were transfected into NIH-3T3 cells, and sorted cells were analyzed by (**C**) polymerase chain reaction (PCR) using a forward primer that anneals upstream of exon 3 and a reverse primer that anneals downstream of exon 3 shows a successful deletion of 275 bp. **D**, Sanger sequencing of a purified PCR product from sorted NIH-3T3 cells transfected with both sgRNAs shows expected deleted region. The effect of exon deletion in sorted NIH-3T3 cells was assessed by *Sav1* (**E**) mRNA analysis by quantitative reverse transcription (qRT)-PCR and (**F**) protein expression by Western blotting. Data were normalized to *Gapdh*. n=3 replicates per group. **G**, Schematic of in vivo study outline and sgRNA vector incorporated into adeno-associated virus serotype 9 (AAV9). **H**, PCR using a forward primer that anneals upstream of exon 3 and a reverse primer that anneals downstream of exon 3 on ventricular+septum homogenates. **I**, Heart weight/tibia length (HW/TL). **J**, Expression of proliferative and hypertrophic genes in dual sg*Sav1*-edited mice. **K**, The effect of exon deletion on cardiac *Sav1* mRNA expression by qRT-PCR analysis and (**L**–**M**) SAV1 protein expression by Western blotting. **N**, Positive regulation of *Sav1* downstream targets by qRT-PCR analysis of mRNA expression. Data are represented as the mean±SEM. **P*<0.05, ***P*<0.01, ****P*<0.001. n=7 to 8 mice per group.

infected and received the sgRNA (Online Figure IX). This is in line with the study by Carroll et al.[13] By in-depth DNA sequencing analysis, we determined that only ≈4% to 15% were efficiently edited by a single sgRNA. If we assume that cardiomyocytes constitute a third of the DNA content in the heart, the percentage of edited cells estimated by DNA sequencing is ≈45%, given that Cas9 is only active in cardiomyocytes. This suggests that a population of cardiomyocytes may be resilient toward editing, and we speculate that this may be related to reduction in chromatin accessibility in postmitotic cells. Higher

Downloaded from http://circres.ahajournals.org/ by guest on February 6, 2018

viral doses increased the sgRNA expression within cells, which may increase the probability that the DNA is cut by Cas9. Despite successful detection of DNA DSB and a subsequent reduction in transcript expression, we were unable to detect a change in protein expression for *Tbx20* and *Sav1* using a single sgRNA. In contrast, for *Myh6*, we observed a reduction in protein expression. However, it is unclear whether the reduction in MYH6 protein expression is directly related to cardiac editing or a secondary effect to heart failure. Importantly, MYH6 is only expressed in cardiomyocytes, and thus the detected reduction in protein expression is a direct reflection of cardiomyocyte protein expression, whereas *Tbx20* and *Sav1* are expressed ubiquitously in the heart. There are several other potential explanations for the absence of an effect of protein expression for *Tbx20* and *Sav1*. First, CRISPR/Cas9 may mediate monoallelic targeting versus biallelic targeting, allowing for compensatory translation mediated by the intact allele. Although AAV9 is highly infectious, it does not integrate into the genome[30] and will therefore be gradually diluted by each subsequent cell division. Neonatal cardiomyocytes do retain some proliferative capacity; however, it is generally accepted that shortly after birth, cardiomyocytes withdraw from the cell cycle.[35] Because our results indicated a high level of sgRNA expression 2 weeks after administration together with the constitutive expression of Cas9, it seems unlikely that biallelic targeting does not occur within targeted cells. Second, the proteins half-life may maintain its abundance within cells for longer periods, although incubations (up to 8 weeks) did not reduce protein expression.

DNA repair by nonhomologous end joining ultimately determines the subsequent outcome of the DNA DSB, resulting in variances in the relative percentage of in-frame and out-of-frame mutations. Here, we observed target-dependent indels that were highly consistent across mice at different ages for the targeted loci (Figures 4 and 6). Although the indel pattern was previously thought to be random, our data support a recent study that showed that the repair profile is related to the unique protospacer sequence,[36] making it possible to design sgRNAs that predominantly produce out-of-frame mutations. However, to maximize the percentage of edited cells, our results strongly suggest the application of a dual sgRNA strategy, and importantly the sgRNAs need to be transcribed from the same vector. The improved efficiency of our dual sgRNA approach in vivo compared with either a single sgRNA or with 2 sgRNAs delivered from 2 vectors suggests that the lack of an effect with a single sgRNA is not because of the selection of inefficient sgRNAs. Although using a dual sgRNA approach is still likely to result in a mosaic pattern of gene disruption, it will increase the percentage of cells in which the gene is successfully mutated.

Conclusions/Future Directions

With the opportunity to express Cas9 within specific tissues by using tissue-specific promoters and the availability of a plethora of delivery vectors, including AAV, lentivruses, hydrodynamic fluids, vesicles, and nanoparticles, to deliver sgRNAs, the ability to study genes in a robust and timely fashion using CRISPR/Cas9 seems promising. However, our results highlight important limitations of using CRISPR/Cas9 to study postnatal cardiac gene function when a high level of gene disruption is required to induce a phenotypic effect. We underscore the usefulness of using dual sgRNAs because this improves precise genome editing. We would, therefore, recommend the design of sgRNAs that flank exons encoding important domains of the protein. Further optimization of cardiac CRISPR/Cas9 to perform gene editing will be required to increase the fidelity of this system to study the effects of gene knockdown on cardiac function in vivo.

Acknowledgments

We acknowledge Lennart Kester for assisting with the DNA sequencing protocol, Jeroen Korving for performing the zygote injections for the generation of myosin heavy chain 6 (Myh6)-CRISPR-associated protein 9 transgenic mice and histological support, Kees Jan Boogerd for identification of open chromatin sites, and Maarten Hoppenbrouwers for his technical assistance. We thank Anko de Graaff and the Hubrecht Imaging Center for supporting the imaging and the Hubrecht Institute animal facilities. We also thank Prof Eric Olson and his laboratory (University of Texas Southwestern Medical Center) for generating the *Myh6* short guide RNA cloning vectors and granting us permission to use it in our studies. Finally, we thank Jose Gomez-Arroyo (University of Cincinnati) for reviewing and editing the article and for graphics.

Sources of Funding

This study was funded by the Foundation Leducq (14CVD04) and the European Research Council (ERC CoG 615708 MICARUS).

Disclosures

E. van Rooij is scientific co-founder and SAB member of miRagen Therapeutics, Inc.

References

1. Yang H, Wang H, Jaenisch R. Generating genetically modified mice using CRISPR/Cas-mediated genome engineering. *Nat Protoc*. 2014;9:1956–1968. doi: 10.1038/nprot.2014.134.
2. Doyle A, McGarry MP, Lee NA, Lee JJ. The construction of transgenic and gene knockout/knockin mouse models of human disease. *Transgenic Res*. 2012;21:327–349. doi: 10.1007/s11248-011-9537-3.
3. Doetschman T, Azhar M. Cardiac-specific inducible and conditional gene targeting in mice. *Circ Res*. 2012;110:1498–1512. doi: 10.1161/CIRCRESAHA.112.265066.
4. Koitabashi N, Bedja D, Zaiman AL, Pinto YM, Zhang M, Gabrielson KL, Takimoto E, Kass DA. Avoidance of transient cardiomyopathy in cardiomyocyte-targeted tamoxifen-induced MerCreMer gene deletion models. *Circ Res*. 2009;105:12–15. doi: 10.1161/CIRCRESAHA.109.198416.
5. Jinek M, Chylinski K, Fonfara I, Hauer M, Doudna JA, Charpentier E. A programmable dual-RNA-guided DNA endonuclease in adaptive bacterial immunity. *Science*. 2012;337:816–821. doi: 10.1126/science.1225829.
6. Anders C, Niewoehner O, Duerst A, Jinek M. Structural basis of PAM-dependent target DNA recognition by the Cas9 endonuclease. *Nature*. 2014;513:569–573. doi: 10.1038/nature13579.
7. Mali P, Yang L, Esvelt KM, Aach J, Guell M, DiCarlo JE, Norville JE, Church GM. RNA-guided human genome engineering via Cas9. *Science*. 2013;339:823–826. doi: 10.1126/science.1232033.
8. Cong L, Ran FA, Cox D, Lin S, Barretto R, Habib N, Hsu PD, Wu X, Jiang W, Marraffini LA, Zhang F. Multiplex genome engineering using CRISPR/Cas systems. *Science*. 2013;339:819–823. doi: 10.1126/science.1231143.
9. Xue W, Chen S, Yin H, Tammela T, Papagiannakopoulos T, Joshi NS, Cai W, Yang G, Bronson R, Crowley DG, Zhang F, Anderson DG, Sharp PA, Jacks T. CRISPR-mediated direct mutation of cancer genes in the mouse liver. *Nature*. 2014;514:380–384. doi: 10.1038/nature13589.
10. Ding Q, Strong A, Patel KM, Ng SL, Gosis BS, Regan SN, Cowan CA, Rader DJ, Musunuru K. Permanent alteration of PCSK9 with in vivo CRISPR-Cas9 genome editing. *Circ Res*. 2014;115:488–492. doi: 10.1161/CIRCRESAHA.115.304351.

Downloaded from http://circres.ahajournals.org/ by guest on February 6, 2018

11. Platt RJ, Chen S, Zhou Y, et al. CRISPR-Cas9 knockin mice for genome editing and cancer modeling. *Cell*. 2014;159:440–455. doi: 10.1016/j.cell.2014.09.014.
12. Sánchez-Rivera FJ, Papagiannakopoulos T, Romero R, Tammela T, Bauer MR, Bhutkar A, Joshi NS, Subbaraj L, Bronson RT, Xue W, Jacks T. Rapid modelling of cooperating genetic events in cancer through somatic genome editing. *Nature*. 2014;516:428–431. doi: 10.1038/nature13906.
13. Carroll KJ, Makarewich CA, McAnally J, Anderson DM, Zentilin L, Liu N, Giacca M, Bassel-Duby R, Olson EN. A mouse model for adult cardiac-specific gene deletion with crispr/cas9. *Proc Natl Acad Sci U S A*. 2016;113:338–343.
14. Xie C, Zhang YP, Song L, et al. Genome editing with CRISPR/Cas9 in postnatal mice corrects PRKAG2 cardiac syndrome. *Cell Res*. 2016;26:1099–1111. doi: 10.1038/cr.2016.101.
15. Guo Y, VanDusen NJ, Zhang L, Gu W, Sethi I, Guatimosim S, Ma Q, Jardin BD, Ai Y, Zhang D, Chen B, Guo A, Yuan GC, Song LS, Pu WT. Analysis of cardiac myocyte maturation using CASAAV, a platform for rapid dissection of cardiac myocyte gene function in vivo. *Circ Res*. 2017;120:1874–1888. doi: 10.1161/CIRCRESAHA.116.310283.
16. Tabebordbar M, Zhu K, Cheng JKW, Chew WL, Widrick JJ, Yan WX, Maesner C, Wu EY, Xiao R, Ran FA, Cong L, Zhang F, Vandenberghe LH, Church GM, Wagers AJ. In vivo gene editing in dystrophic mouse muscle and muscle stem cells. *Science*. 2016;351:407–411. doi: 10.1126/science.aad5177.
17. Nelson CE, Hakim CH, Ousterout DG, Thakore PI, Moreb EA, Castellanos Rivera RM, Madhavan S, Pan X, Ran FA, Yan WX, Asokan A, Zhang F, Duan D, Gersbach CA. In vivo genome editing improves muscle function in a mouse model of Duchenne muscular dystrophy. *Science*. 2016;351:403–407. doi: 10.1126/science.aad5143.
18. Long C, Amoasii L, Mireault AA, McAnally JR, Li H, Sanchez-Ortiz E, Bhattacharyya S, Shelton JM, Bassel-Duby R, Olson EN. Postnatal genome editing partially restores dystrophin expression in a mouse model of muscular dystrophy. *Science*. 2016;351:400–403. doi: 10.1126/science.aad5725.
19. Swiech L, Heidenreich M, Banerjee A, Habib N, Li Y, Trombetta J, Sur M, Zhang F. In vivo interrogation of gene function in the mammalian brain using CRISPR-Cas9. *Nat Biotechnol*. 2015;33:102–106. doi: 10.1038/nbt.3055.
20. Hsu PD, Scott DA, Weinstein JA, Ran FA, Konermann S, Agarwala V, Li Y, Fine EJ, Wu X, Shalem O, Cradick TJ, Marraffini LA, Bao G, Zhang F. DNA targeting specificity of RNA-guided Cas9 nucleases. *Nat Biotechnol*. 2013;31:827–832. doi: 10.1038/nbt.2647.
21. Ran FA, Hsu PD, Wright J, Agarwala V, Scott DA, Zhang F. Genome engineering using the CRISPR-Cas9 system. *Nat Protoc*. 2013;8:2281–2308. doi: 10.1038/nprot.2013.143.
22. Arsic N, Zentilin L, Zacchigna S, Santoro D, Stanta G, Salvi A, Sinagra G, Giacca M. Induction of functional neovascularization by combined VEGF and angiopoietin-1 gene transfer using AAV vectors. *Mol Ther*. 2003;7:450–459.
23. Junker JP, Noël ES, Guryev V, Peterson KA, Shah G, Huisken J, McMahon AP, Berezikov E, Bakkers J, van Oudenaarden A. Genome-wide RNA tomography in the zebrafish embryo. *Cell*. 2014;159:662–675. doi: 10.1016/j.cell.2014.09.038.
24. Shen T, Aneas I, Sakabe N, et al. Tbx20 regulates a genetic program essential to adult mouse cardiomyocyte function. *J Clin Invest*. 2011;121:4640–4654. doi: 10.1172/JCI59472.
25. Heallen T, Morikawa Y, Leach J, Tao G, Willerson JT, Johnson RL, Martin JF. Hippo signaling impedes adult heart regeneration. *Development*. 2013;140:4683–4690. doi: 10.1242/dev.102798.
26. Heallen T, Zhang M, Wang J, Bonilla-Claudio M, Klysik E, Johnson RL, Martin JF. Hippo pathway inhibits Wnt signaling to restrain cardiomyocyte proliferation and heart size. *Science*. 2011;332:458–461. doi: 10.1126/science.1199010.
27. Lu L, Li Y, Kim SM, Bossuyt W, Liu P, Qiu Q, Wang Y, Halder G, Finegold MJ, Lee JS, Johnson RL. Hippo signaling is a potent in vivo growth and tumor suppressor pathway in the mammalian liver. *Proc Natl Acad Sci U S A*. 2010;107:1437–1442.
28. Stennard FA, Costa MW, Lai D, Biben C, Furtado MB, Solloway MJ, McCulley DJ, Leimena C, Preis JI, Dunwoodie SL, Elliott DE, Prall OW, Black BL, Fatkin D, Harvey RP. Murine T-box transcription factor Tbx20 acts as a repressor during heart development, and is essential for adult heart integrity, function and adaptation. *Development*. 2005;132:2451–2462. doi: 10.1242/dev.01799.
29. Lovric J, Mano M, Zentilin L, Eulalio A, Zacchigna S, Giacca M. Terminal differentiation of cardiac and skeletal myocytes induces permissivity to AAV transduction by relieving inhibition imposed by DNA damage response proteins. *Mol Ther*. 2012;20:2087–2097. doi: 10.1038/mt.2012.144.
30. Zacchigna S, Zentilin L, Giacca M. Adeno-associated virus vectors as therapeutic and investigational tools in the cardiovascular system. *Circ Res*. 2014;114:1827–1846. doi: 10.1161/CIRCRESAHA.114.302331.
31. Camelliti P, Borg TK, Kohl P. Structural and functional characterisation of cardiac fibroblasts. *Cardiovasc Res*. 2005;65:40–51. doi: 10.1016/j.cardiores.2004.08.020.
32. Jones WK, Grupp IL, Doetschman T, Grupp G, Osinska H, Hewett TE, Boivin G, Gulick J, Ng WA, Robbins J. Ablation of the murine alpha myosin heavy chain gene leads to dosage effects and functional deficits in the heart. *J Clin Invest*. 1996;98:1906–1917. doi: 10.1172/JCI118992.
33. Knight SC, Xie L, Deng W, Guglielmi B, Witkowsky LB, Bosanac L, Zhang ET, El Beheiry M, Masson JB, Dahan M, Liu Z, Doudna JA, Tjian R. Dynamics of CRISPR-Cas9 genome interrogation in living cells. *Science*. 2015;350:823–826. doi: 10.1126/science.aac6572.
34. Yue F, Cheng Y, Breschi A, et al; Mouse ENCODE Consortium. A comparative encyclopedia of DNA elements in the mouse genome. *Nature*. 2014;515:355–364. doi: 10.1038/nature13992.
35. Soonpaa MH, Kim KK, Pajak L, Franklin M, Field LJ. Cardiomyocyte DNA synthesis and binucleation during murine development. *Am J Physiol*. 1996;271:H2183–H2189.
36. van Overbeek M, Capurso D, Carter MM, Thompson MS, Frias E, Russ C, Reece-Hoyes JS, Nye C, Gradia S, Vidal B, Zheng J, Hoffman GR, Fuller CK, May AP. DNA repair profiling reveals nonrandom outcomes at Cas9-mediated breaks. *Mol Cell*. 2016;63:633–646. doi: 10.1016/j.molcel.2016.06.037.

Downloaded from http://circres.ahajournals.org/ by guest on February 6, 2018

Circulation Research
JOURNAL OF THE AMERICAN HEART ASSOCIATION

American Heart Association®

Postnatal Cardiac Gene Editing Using CRISPR/Cas9 With AAV9-Mediated Delivery of Short Guide RNAs Results in Mosaic Gene Disruption

Anne Katrine Johansen, Bas Molenaar, Danielle Versteeg, Ana Rita Leitoguinho, Charlotte Demkes, Bastiaan Spanjaard, Hesther de Ruiter, Farhad Akbari Moqadam, Lieneke Kooijman, Lorena Zentilin, Mauro Giacca and Eva van Rooij

Circ Res. 2017;121:1168-1181; originally published online August 29, 2017;
doi: 10.1161/CIRCRESAHA.116.310370
Circulation Research is published by the American Heart Association, 7272 Greenville Avenue, Dallas, TX 75231
Copyright © 2017 American Heart Association, Inc. All rights reserved.
Print ISSN: 0009-7330. Online ISSN: 1524-4571

The online version of this article, along with updated information and services, is located on the World Wide Web at:
http://circres.ahajournals.org/content/121/10/1168

Data Supplement (unedited) at:
http://circres.ahajournals.org/content/suppl/2017/08/29/CIRCRESAHA.116.310370.DC1

Permissions: Requests for permissions to reproduce figures, tables, or portions of articles originally published in *Circulation Research* can be obtained via RightsLink, a service of the Copyright Clearance Center, not the Editorial Office. Once the online version of the published article for which permission is being requested is located, click Request Permissions in the middle column of the Web page under Services. Further information about this process is available in the Permissions and Rights Question and Answer document.

Reprints: Information about reprints can be found online at:
http://www.lww.com/reprints

Subscriptions: Information about subscribing to *Circulation Research* is online at:
http://circres.ahajournals.org//subscriptions/

Downloaded from http://circres.ahajournals.org/ by guest on February 6, 2018

Data Supplement I

Materials and Methods

Animals

All experiments were carried out in accordance with the guidelines of the Animal Welfare Committee of the Royal Netherlands Academy of Arts and Sciences. To generate an organ-restricted Cas9 mouse, homozygous Cre dependent Rosa26-Cas9 mice (B6;129-Gt(ROSA)26Sortm1(CAG-cas9*,-EGFP)Fezh/J; stock number 024857, obtained from Jackson Labs, Germany, which were originally generated on a C57/BL6N background) were crossed with *Myh6*-Cre transgenic (tg) mice (Cre expression driven by a cardiomyocyte-specific promoter; a generous gift from Jeffery Molkentin, Cincinnati Children's Hospital Medical Center, bred on a C57/BL6N background) to generate $Myh6^{Cas9}$ mice. For all experiments, Cre negative littermates were used as a control.

To generate transgenic mice with Cas9 expression driven by the cardiomyocyte specific promoter, *Myh6*, we PCR amplified 3XFLAG-Cas9 from the plasmid pX330-U6-Chimeric_BB-CBh-hSpCas9, a gift from Feng Zhang (Addgene plasmid # 42230), using primers with added restriction sites SalI and HindIII (see *data supplement S2* for primer sequences). The resulting product was purified and inserted into SalI and HindIII digested pJG/ALPHA MHC, a gift from Jeffrey Robbins (Addgene plasmid # 55594), containing the last exon of Myh7, an intergenic region and first 3 non-coding exons of *Myh6* upstream of the inserted Cas9 and a human growth hormone polyA (hGHpA) sequence downstream. Construct insertion was determined by restriction digestion and sequencing. The *Myh6*-3XFLAG-Cas9-hGHpA plasmid was linearized by restriction digestion using NotI followed by gel extraction and purification using the Tube-O-Dialyzer kit (G biosciences, VWR International B.V, Amsterdam, The Netherlands) according to manufacturer's instructions. The sample was diluted to 2ng/µl and injected into zygotes of F_1 C57/BL6/CBA mice. Founder mice (F_0) were identified by ear biopsy genotyping. From 50 animals, 1 F_0 mouse was identified which was bred with C57/BL6 mice. *See data supplement S3 for plasmid map.*

Animal numbers used

For the specific number of animals used per experiment, refer to figure legends. For the evaluation of the effect of Cas9 expression in adult mice, a total of 7 mice were analysed per group. To evaluate the effect of sgRNA mediated Cas9 disruption by intra-peritoneal (i.p) injection, 3-10 mice were analysed per group. To evaluate the effect of sgRNA mediated Cas9 disruption by intra-cardiac injection, 5-7 mice were analysed per group.

sgRNA Design

We designed sgRNAs for SpCas9 target selection using the CRISPR design tool (http://crispr.mit.edu/), which systematically screens for off-target (OT) effects[1]. The 20-nucleotide sequences were designed to precede a CRISPR type II specific protospacer adjacent motif (PAM) sequence 5'–NGG. sgRNA sequences are listed in *data supplement S2*.

sgRNA Constructs and Transfection

Single stranded sgRNA sequences were annealed and cloned into pSpCas9(BB)-2A-Puro (PX459) following restriction digestion with Bbs1 (PX459 was a gift from Feng Zhang (Addgene plasmid # 48139)).[2] Successful cloning was confirmed by double digestion with BbsI and AgeI. To determine functionality of sgRNA, sgRNA-PX459 vectors were transfected into 30% confluent NIH-3T3 cells (Hubrecht Institute Cell Bank) in 6 well plates using Lipofectamine 3000 (Invitrogen; Fisher Scientific, Landsmeer, The Netherlands) according to manufacturer's instructions, with slight modifications. Briefly, 2.5µg plasmid

DNA and 2.5µl Lipofectamine 3000 was diluted in 100µl Opti-Mem (Fisher Scientific). To the DNA sample, 2.5µl of p3000 was added. Samples were combined and incubated for 10 mins and then added drop-wise to each well. For dual guide experiments, 2.5µg of plasmid DNA was added for each vector. 24 hours later, cells were sorted for puromycin resistance in medium containing 2.5µg/ml puromycin for 48 hours. Cell culture medium was replaced and cells were grown for an additional 48 hours prior to cell harvest and genomic DNA extraction using the DNeasy Blood and Tissue kit (QIAGEN Benelux B.V., Venlo, The Netherlands) according to manufacturer's instructions, RNA isolation and protein isolations (see below).

T7 Endonuclease (T7E1) Assay and Indel Analysis

Genomic DNA was amplified with Taq Roche DNA polymerase (Sigma-Aldrich, Zwijndrecht, The Netherlands) using primers against the modified locus and the top four potential gene-coding off-targets (see *data supplement S2* for a list of primers). Indel formation was determined using the T7E1 assay, according to manufacturer's instructions (New England Biolabs (NEB), Bioké, Leiden, The Netherlands), with slight modifications. Briefly, 150ng of DNA was PCR amplified and then denatured at 95°C and re-annealed by reducing the temperature by 5°C/minute. The resulting product was incubated with T7E1 at a concentration of 0.07units/µl for 30 minutes and then separated on a 1.5% agarose gel. Band intensity quantification (indel analysis) was performed as previously described[2]. Briefly, indel frequency was calculated using the formula indel (%) = 100 x $(1-\sqrt{(1-f_{cut})})$, where $f_{cut}=(b+c)/(a+b+c)$, where a is the integrated density of the undigested PCR product and b and c are the integrated densities of the cleaved PCR products.

AAV9 DNA Vectors

The sgRNA that appeared the most efficient at inducing DNA strand breaks by *in vitro* T7E1 assay were cloned into an AAV vector with an expression cassette for Renilla luciferase and the sgRNA backbone - AAV:ITR-U6-sgRNA(backbone)-pEFS-Rluc-2A-Cre-WPRE-hGHpA-ITR was a gift from Feng Zhang (Addgene plasmid # 60226)[3] which was modified to exclude Cre by restriction digestion with NheI and HindIII (NEB) and recombined using the forward (5′-CTAGCGGAAGCGGAGATATCA-3′) and reverse (5′-AGCTTGATATCTCCGCTTCCG-3′) primers. Sanger sequencing confirmed successful removal of Cre using a primer located upstream of the Cre coding sequence (5′-CCAATGCTATTGTTGAAGGTGCC -3′). *See data supplement S3 for plasmid map.* To generate a dual sgRNA vector, we PCR amplified the U6-sgRNA(backbone) from the plasmid # 60226 with the inserted sgRNA targeting the 3′ end of the gene using the forward primer with a Xba1 restriction site:

(GCTCTAGAGAGGGCCTATTTCCCATGATTCCTTCATA)

And the reverse primer with a Kpn1 restriction site:

(GCGGTACCAAAAAAGCACCGACTCGGTGCC).

We digested the destination plasmid (#60226 with the sgRNA targeting the 5′ end) and the resulting PCR product with Kpn1 and Xba1 and ligated the PCR product into the vector for transformation. We confirmed sequence insertion by restriction digestion and sequencing using primers identical to the sgRNA insert sequence.

AAV9 Production

Recombinant AAV vectors used in this study were generated by the AAV Vector Unit at ICGEB Trieste (http://www.icgeb.org/avu-core-facility.html) as described previously[4]. Briefly, HEK293T cells were co-transfected with a triple-plasmid for packaging of AAV of serotype 9. Viral stocks were obtained by $CsCl_2$ gradient centrifugation and titration of AAV viral particles was determined by qRT-PCR for quantification of viral genomes (vg), as

described previously [5]. The AAV9 vector encoding *Myh6* was a gift from Eric Olson and the ICGEB[6]. The viral preparations had titers between $3.0x10^{12}$ and $1.3x10^{14}$ vg/ml.

Injection of AAV Vectors into Neonatal mice

Neonatal mice were genotyped at postnatal day 2 (P2) using the Phire Animal Tissue Direct PCR Kit (Fisher Scientific) according to manufacturer's instructions. At P3 or P10 heterozygous or homozygous *Myh6*^{Cas9} mice or their littermate controls (*Myh6*-Cre negative) were injected with AAV9-sgRNA at either a dose of 5×10^{11} (low dose; LD), 1×10^{12} (medium dose; MD) or 2.5×10^{12} (high dose, HD) viral genomes (vg) per animal by intra-peritoneal (i.p) injection. For dual sgRNA delivery using two viral vectors, the 3′ and 5′ guides were mixed in equal units of vg and administered at a final multiplicity of infection (MOI) of 2.5×10^{12} vg per animal by i.p. injection. For dual sgRNA delivery with the same vector, a medium dose was used (this was the maximum dose that could be achieved with the viral titer obtained). Animals were sacrificed and organs isolated 2, 4, 6 or 8 weeks post exposure. All experiments were done blindly – the genotype of the mice was not known to the researcher injecting the mice and we did not uncover the genotype of the mice until after qRT-PCR analysis. A total of 4-10 mice were used per group.

Intracardiac AAV9 Delivery

Mice were anesthetized with a low dose mixture of ketamine (60mg/kg) and xylazine (7mg/kg) by i.p. injection and intubated with a tracheal tube connected to a ventilator. Mice were supplemented and maintained under anesthesia with 1.5% isoflurane. A surgical plane of anesthesia was confirmed by a lack of a pain reflex. To expose the heart, the skin was incised at the third intercostal space, followed by retraction of the pectoral muscles and intercostal muscles. The free wall of the left ventricle was injected with a HD of AAV9-sg*Sav1* in 2 locations (total volume per injection was 6 µl). The muscle and rib cage was closed with 5-0 silk suture and analgesia (buprenorphine, 0.05-0.1mg/kg) were given immediately after surgery and as necessary. A total of 5-7 mice were analysed per group.

Echocardiography

Cardiac function was determined by two-dimensional transthoracic echocardiography on sedated mice (2-2.5% isoflurane). This analysis was performed with a Visual Sonic Ultrasound system with a 30 MHz transducer. The heart was imaged in a parasternal short-axis view at the level of the papillary muscles, to record M-mode measurements, determine heart rate, wall thickness, and end-diastolic and end-systolic dimensions. % Ejection fraction (EF) was measured as an index of contractile function and was calculated automatically by the software.

Tissue Harvest

At sacrifice, whole hearts were excised from the chest cavity and cleared of blood with ice-cold PBS. Whole hearts (atria + ventricles) were weighed to obtain the heart weight (HW) to determine hypertrophy by expressing the HW over the body weight (BW) and tibia length (TL). The atria's were subsequently removed and the ventricles (right and left) were cut for DNA, RNA and protein analysis. In addition, the lung, liver, spleen and kidney were isolated for off-target analysis. For intra-cardiac injections, the injected myocardium was specifically isolated, cut into small pieces and divided for DNA, RNA and protein analysis.

RNA and DNA isolation

Total RNA and DNA was purified from isolated organs with TRIzol reagent (Fisher Scientific) according to manufacturer's instructions. One microgram of RNA was reverse transcribed to synthesize cDNA using iScript Reverse transcriptase kit (Bio-Rad, Veenendaal, The Netherlands).

qRT-PCR

Quantitative PCR was performed using iQ SYBR Green supermix (Bio-Rad) according to manufacturer's instructions in a CFX96 PCR system. Primer sequences are listed in *data supplement S2*. All values were normalized to Gapdh. Note that in the main figures, the forward primers to identify target disruption were located on the sgRNA cutting site, apart from in **figure 5** where primers were used to detect all isoforms. The reason for this discrepancy was to standardize the protocol with that for the *Myh6* edited mice.

Western Blotting

Cardiac ventricles, lung, liver, kidney and spleen were homogenized in 400µl of ice-cold RIPA buffer supplemented with a cocktail of protease inhibitors (cOmplete, Sigma-Aldrich) followed by ice-solubilization and cell fractioning prior to protein quantification (Bradford Assay, Bio-Rad). For NIH-3T3 isolations, 120µl of RIPA buffer with supplements was used. 40µg (organ lysates) or 10µg (cell lysates) of protein was separated by SDS-PAGE in a 12% acrylamide gel and analysed by Western blotting using antibodies against TBX20 (0.1µg/ml 5% BSA-TBS-T v/v, Santa Cruz Biotechnology, Heidelberg, Germany sc134061), SAV1 (1:1000 5% BSA-TBS-T v/v, Cell Signaling, #13301), FLAG (0.78µg/ml, Sigma, F3165) or eGFP (0.5µg/ml Abnova, MAB1765, The Netherlands). GAPDH (0.2µg/ml 5% milk-TBS-T v/v Millipore) was used as the internal loading control and for quantification analysis. Blots were imaged with a ImageQuant Las4000 scanner (GE Healthcare Life Sciences).

For the specific detection of MYH6 protein, we extracted antibody from a B lymphocyte cell line, BA-G5 (ATCC®HB27™, Rockville, USA) derived from spleen cells of animals immunized with bovine fetal skeletal muscle myosin. All immunoblots were incubated with medium from 1 x 10^6 cells/mL.

To isolate nuclear and cytoplasmic fractions for determination of Cas9 localization, we used a previously published protocol[7], with minor modifications. Briefly, we excised the heart, rinsed in PBS, cut into small pieces and homogenized on ice using a tissue grinder in 2mL of lysis buffer 10mM Tris pH 7.5, 15mM NaCl, and 0.15% Nonidet P-40 in deionized water with protease inhibitors. The lysate was poured through a 100µm strainer and centrifuged at 4,0000 rpm for 5 minutes at 4°C. The resulting supernatant is the cytosolic fragment. The nuclear pellet was resuspended in 500µl lysis buffer and layered on top of 1ml of sucrose buffer (24% sucrose weight/volume, 10mM Tris pH 7.5, and 15mM NaCl in deionized water with protease inhibitor) and centrifuged at 5,000 rpm for 10 minutes at 4°C. The supernatant was discarded and the resultant nuclear pellet was rinsed once with PBS and then resuspended in 200µl detergent extraction buffer (20mM HEPES pH 7.6, 7.5mM $MgCl_2$. 0.2mM EDTA, 30mM NaCl, 1M Urea, 1% NP-40 in deionized water with protease inhibitors. To determine the purity of the fractions, we used antibodies against histone H3 (nucleus; 1µg/ml 5% BSA-TBS-T v/v, Abcam, ab1719, I.T.K. Diagnostics, The Netherlands) and α-tubulin (cytoplasmic; 4.72µg/ml 5% BSA-TBS-T v/v, Sigma T5168).

Next Generation Sequencing and Indel Analysis

For sequencing analysis of indels, we prepared cardiac genomic DNA libraries using customized barcoding methods as described by Junker *et al*.[8] To generate the library, a low-cycle PCR using the Q5® High-Fidelity 2X Master Mix (NEB) on 60ng genomic DNA was performed to amplify and barcode the target site using forward primers with a partial 5′ Illumina adapter and reverse primers with a 3′ Illumina adaptor, with a unique barcode sequence present in either the forward or the reverse primer (See *data supplement S2* for primer sequences). The PCR primer locations were designed so that the indel mutations can be identified within either the right mate or the left mate. For the sequencing experiments where the mutations are present in the right mate read (from the 3′ primer), the forward primer was located 238 to 217 base pairs upstream of the sgRNA cut site for *Sav1*, 244 to 223

base pairs for *Tbx20* and 218 to 199 base pairs for *Myh6*. The reverse primer was located 16 to 35 base pairs downstream of the gRNA cut site for *Sav1*, 30 to 48 base pairs for *Tbx20* and 18 to 39 base pairs for *Myh6*. For the sequencing experiments where the mutations are present in the left mate read (from the 5′ primer), the forward primer was located 48 to 26 base pairs upstream of the gRNA cut site for *Sav1*, 44 to 26 base pairs for *Tbx20* and 48 to 30 basepairs for *Myh6*. The reverse primer was located 204 to 226 base pairs downstream of the gRNA cut site for *Sav1*, 198 to 223 base pairs for *Tbx20* and 203 to 223 base pairs for *Myh6.* The targeted locus was PCR amplified using as short cycle PCR (9 cycles). Subsequently, barcoded samples were pooled and purified using QIAquick PCR Purification Kit (QIAGEN) followed by 2 bead cleanups using The Agencourt AMPure XP system (Beckman Coulter, Brea USA), all according to manufacturer's instructions. A second round library preparation PCR was performed using a 5′ and 3′ primer containing the remaining Illumina adaptor sequences (See *data supplement S2* for primer sequences). PCR amplification was performed using a short cycle PCR (12 cycles) and purified as previously described prior to sequencing.

The Illumina NextSeq 500/550 High-Output v2 Kit (150 cycles) was used for sequencing. Strand-specific paired-end base-pair reads were generated on an Illumina NextSeq 500 to obtain a left mate read (from the 5′ primer) and a right mate read (from the 3′ primer). The sequencing data was mapped to *Sav1*, *Tbx20* and *Myh6* using bwa mem 0.7.10. We first selected for reads that had lengths of 74, 75 or 76 base pairs, as this constituted at least 95% of all reads mapped to the genes. For the experiments where the mutations could be identified in the right mate read, reads were analysed if the left mate was mapped in the forward direction and contained the correct barcode and if the right mate was mapped in the reverse direction and started with the primer sequence. For the experiments where the mutations could be identified in the left mate read, reads were analysed if the left mate was mapped in the forward direction and started with the primer sequence and if the right mate was mapped in the reverse direction and contained the barcode sequence. For all experiments, the read containing the barcode was only used for sample identification and the complementary read was used for alignment. To identify indels, we first classified right mate reads using the CIGAR string, which describes the length and position of the indels in the alignment, combined with the 3′ location of the right mate. Within each CIGAR string we performed a sub-classification based on which sequences it contained. We retained CIGAR strings for which we saw at least 20 reads in a library and that made up at least 5% of all reads in its CIGAR-class. We next discarded all CIGAR strings that contained partial soft-clipped part(s) in combination with partial mapped parts that had wild-type sequences. This was done because it was not possible to determine for these CIGAR strings whether it depicted a wild-type sequence or a mutant sequence that contained a mutation in the soft-clipped part(s) of the read. We divided the remaining CIGAR strings in subgroups based on the total amount of base pair shifts in the reading frame resulting from all indels combined. For each base-pair shift, we calculated the percentage of reads belonging to all CIGAR strings with the corresponding base-pair shift relative to the total number of reads. The total number of reads that were used for the analysis was between 1.9 and 0.18 million reads. Except for a NGS experiment on one *Myh6* sample, where the number of reads was 7000. However, results in this sample were comparable to the results of the NGS experiment on the other *Myh6* samples.

Immunohistochemistry

Whole heart samples were fixed in 4% paraformaldehyde, embedded in paraffin and cut into 4µm sections. Sections were dewaxed and rehydrated through an ethanol to water gradient and antigen retrieval was performed in boiling 10 mmol/L Tris-EDTA with 0.05% tween for 20 minutes followed by a cool down period of 30 minutes. Non-specific binding was blocked with 1% BSA in PBS for 1 hour at room temperature. Sections were incubated overnight with antibodies against eGFP (20µg/ml, GFP-1010, Aves) or TBX20 (2µg/ml, Allele Biotechnology, ABP-PAB-11248) and sarcomeric alpha actinin (ACTN2, 1:400,

HPA008315, Sigma-Aldrich) in 1% BSA-TBS-T v/v. Excess primary antibody was washed off in 3 x PBS washes and sections were incubated with ALEXA-flour secondary antibodies (anti-chicken 488 for GFP and anti-rabbit 568 for ACTN2). Nuclei were stained with DAPI and sections were mounted for confocal imaging. Hematoxylin and eosin stains were performed using standard protocols.

To image ZsGreen expression, we preserved the fluorescence by fixation in a low percentage paraformaldehyde buffer (1% paraformaldehyde, 0.2% $NaIO_4$, 61mM Na_2HPO_4, 75mM L-Lysine and 14 mM NaH_2PO_4 in H_2O) overnight at 4°C. After fixation, organs were placed in a 30% sucrose solution (w/v) overnight prior to embedding in Tissue Freezing Medium (Leica Microsystems Nussloch GmbH, Germany). 10µm sections were cut using a Leica CM3050 cryotome, dried and mounted for imaging.

Imaging Equipment

All confocal imaging was acquired using a Leica SP8 Confocal Microscope (**Figure 1C** and **Figure S9B**). For tilescans of histological sections, we used a Leica DM4000 (**Figure 5H**). For stereoimaging of the hearts we used a Leica M165 FC fluorescence stereomicroscope (**Figure S9A**).

Statistics

Data was plotted and analysed using GraphPad Prism. Data were expressed as mean ± SEM. Data was analysed using a student's t test. $P<0.05$ was considered statistically significant.

Reference List

1. Hsu PD, Scott DA, Weinstein JA, Ran FA, Konermann S, Agarwala V, Li Y, Fine EJ, Wu X, Shalem O, Cradick TJ, Marraffini LA, Bao G, Zhang F. DNA targeting specificity of rna-guided cas9 nucleases. *Nature biotechnology*. 2013;31:827-832

2. Ran FA, Hsu PD, Wright J, Agarwala V, Scott DA, Zhang F. Genome engineering using the crispr-cas9 system. *Nature protocols*. 2013;8:2281-2308

3. Platt RJ, Chen S, Zhou Y, et al. Crispr-cas9 knockin mice for genome editing and cancer modeling. *Cell*. 2014;159:440-455

4. Arsic N, Zentilin L, Zacchigna S, Santoro D, Stanta G, Salvi A, Sinagra G, Giacca M. Induction of functional neovascularization by combined vegf and angiopoietin-1 gene transfer using aav vectors. *Molecular therapy : the journal of the American Society of Gene Therapy*. 2003;7:450-459

5. Zentilin L, Marcello A, Giacca M. Involvement of cellular double-stranded DNA break binding proteins in processing of the recombinant adeno-associated virus genome. *Journal of virology*. 2001;75:12279-12287

6. Carroll KJ, Makarewich CA, McAnally J, Anderson DM, Zentilin L, Liu N, Giacca M, Bassel-Duby R, Olson EN. A mouse model for adult cardiac-specific gene deletion with crispr/cas9. *Proceedings of the National Academy of Sciences of the United States of America*. 2016;113:338-343

7. Franklin S, Zhang MJ, Chen H, Paulsson AK, Mitchell-Jordan SA, Li Y, Ping P, Vondriska TM. Specialized compartments of cardiac nuclei exhibit distinct proteomic anatomy. *Molecular & cellular proteomics : MCP*. 2011;10:M110 000703

8. Junker JP, Noel ES, Guryev V, Peterson KA, Shah G, Huisken J, McMahon AP, Berezikov E, Bakkers J, van Oudenaarden A. Genome-wide rna tomography in the zebrafish embryo. *Cell*. 2014;159:662-675

Data Supplement II

Name	Sequence	Purpose
Tbx20 sgRNA 1 (T1) fwd	GCTGGACATAAGCGCGGCGA (antisense)	*In vitro* and in *vivo* sgRNA
Tbx20 sgRNA 1 (T1) rv	TCGCCGCGCTTATGTCCAGC	*In vitro* and in *vivo* sgRNA
Tbx20 sgRNA 2 (T2) fwd	GCCGCGCTTATGTCCAGCGG (sense)	*In vitro* and in *vivo* sgRNA
Tbx20 sgRNA 2 (T2) rv	CCGCTGGACATAAGCGCGGC	*In vitro* and in *vivo* sgRNA
Tbx20 sgRNA 3 (T3) fwd	ATCGCCGCGCTTATGTCCAG (sense)	*In vitro* and in *vivo* sgRNA
Tbx20 sgRNA 3 (T3) rv	CTGGACATAAGCGCGGCGAT	*In vitro* and in *vivo* sgRNA
Tbx20 sgRNA 4 (T4) fwd	GCCGCCGCTGGACATAAGCG (antisense)	*In vitro* and in *vivo* sgRNA
Tbx20 sgRNA 4 (T4) rv	CGCTTATGTCCAGCGGCGGC	*In vitro* and in *vivo* sgRNA
Sav1 sgRNA 1 (S1) fwd	GGAAGTCCTTCTCGTTCAAG (antisense)	*In vitro* and in *vivo* sgRNA
Sav1 sgRNA 1 (S1) rv	CTTGAACGAGAAGGACTTCC	*In vitro* and in *vivo* sgRNA
Sav1 sgRNA 2 (S2) fwd	AGTCATCCCCTTGAACGAGA (sense)	*In vitro* and in *vivo* sgRNA
Sav1 sgRNA 2 (S2) rv	TCTCGTTCAAGGGGATGACT	*In vitro* and in *vivo* sgRNA
Sav1 sgRNA 3 (S3) fwd	AGAATTTGGAACCTATTACG (sense)	*In vitro* and in *vivo* sgRNA
Sav1 sgRNA 3 (S3) rv	CGTAATAGGTTCCAAATTCT	*In vitro* and in *vivo* sgRNA
Sav1 sgRNA 4 (S4) fwd	AGGAAGTCCTTCTCGTTCAA (antisense)	*In vitro* and in *vivo* sgRNA
Sav1 sgRNA 4 (S4) rv	TTGAACGAGAAGGACTTCCT	*In vitro* and in *vivo* sgRNA
Sav1 exon removal 5′ end fwd	GAGTCACGGCTACATCTCTA (sense)	*In vitro* and in *vivo* sgRNA
Sav1 exon removal 5′ end rv	TAGAGATGTAGCCGTGACTC	*In vitro* and in *vivo* sgRNA
Sav1 exon removal 3′ end fwd	ACCCCTGTGCTCCGAGGTAA (sense)	*In vitro* and in *vivo* sgRNA
Sav1 exon removal 3′ end rv	TTACCTCGGAGCACAGGGGT	*In vitro* and in *vivo* sgRNA
Casp6 fwd	GAGAAGTTTCTGGGGCTGTG	*Sav1* off-target 1 T7E1
Casp6 rv	CAAAAGGGGAGGCAAAGTAG	*Sav1* off-target 1 T7E1
*Acot11*fwd	AAGGTTTTCCAGGGAACCAG	*Sav1* off-target 2 T7E1
Acot11 rv	ATCCGGCATCAACAAGAGAC	*Sav1* off-target 2 T7E1
Tmem2 fwd	TGCACGTGTGTATGTGCAAG	*Sav1* off-target 3 T7E1
Tmem2 rv	CGCAGCCTAGAGAAAGTTGG	*Sav1* off-target 3 T7E1
Osbpl10 fwd	TATGCAACAGCTTGCCTGAC	*Sav1* off-target 4 T7E1
Osbpl10 rv	CAAAACCAGGCCTATTACGG	*Sav1* off-target 4 T7E1
Rab3gap2 fwd	GACAAAACCCCAGCTAGCAC	*Tbx20* off-target 1 T7E1
Rab3gap2 rv	TGGCAGACTCCAGATCAGTG	*Tbx20* off-target 1 T7E1
Scp2 fwd	AGAGAAGACTGCGAGTTGGC	*Tbx20* off-target 2 T7E1
Scp2 rv	ACATTGCTCAAGCAGGGACT	*Tbx20* off-target 2 T7E1
Ttll5 fwd	TGTAGTAACGGGGGAAGCAG	*Tbx20* off-target 3 T7E1
Ttll5 rv	AATCTCCAATTCCCAGGCTTCT	*Tbx20* off-target 3 T7E1
Ptk7 fwd	GTAAGGAGCCGTGAGGTGAG	*Tbx20* off-target 4 T7E1
Ptk7 rv	TGAATGACAGTCCAGCAAGC	*Tbx20* off-target 4 T7E1
Tbx20 exon 1 fwd	ATCGCCGCGCTTATGTCCAGC	qRT-PCR
Tbx20 exon 2 rv	TGTGCACAGAGAGGATGAGG	qRT-PCR
Tbx20 exon 7 fwd	CACCTATGGGGAAGAGGATG	qRT-PCR
Tbx20 exon 8 rv	TGACGATACCCAGGAACTGAG	qRT-PCR
Tbx20 exon 3 fwd	TCTCTGTGCACAGAGCCACTG	qRT-PCR
Tbx20 exon 3/4 rv	CATCCTCCTGCCAGACTTGGT	qRT-PCR

Tbx20 exon 6 fwd	CCGTTTGCCAAAGGATTCCG	qRT-PCR
Tbx20 exon 7 rv	AAAGGCTGATCCTCGACTCTC	qRT-PCR
Tbx20 exon 7 fwd	AACTCAGAGTCGAGGATCAGC	qRT-PCR
Tbx20 exon 8 rv	ATCGGTGTCGCTATGGATGC	qRT-PCR
Sav1 exon 3 fwd	AGTCATCCCCTTGAACGAGA	qRT-PCR
Sav1 exon 4 rv	TTGTGGCTGATACGTGATGG	qRT-PCR
Sav1 exon 4 fwd	TGCAAATCCCTACCATACTGC	qRT-PCR
Sav1 exon 5 rv	AGCATTCCCTGGTACGTGTC	qRT-PCR
Sav1 exon 4 fwd	CCCGAGCCCCTGTGAAATATG	qRT-PCR
Sav1 exon 5 rv	TCAGCATTCCCTGGTACGTG	qRT-PCR
Sav1 exon 1 fwd	ATGCTGTCCCGCAAGAAAAC	qRT-PCR
Sav1 exon 2 rv	GAAGGCATGAGATTCCGCAG	qRT-PCR
Sav1 exon 4 fwd	GGTATGATCAGCCTCCACCC	qRT-PCR
Sav1 exon 5 rv	TGTGGTCATATTTCACAGGGGC	qRT-PCR
Myh6 fwd	GTTAAGGCCAAGGTCGTGTC	qRT-PCR
Myh6 rv	GCCATGTCCTCGATCTTGTC	qRT-PCR
Irx4 fwd	CCTCTGCTCCTCAGTTCCTG	qRT-PCR
Irx4 rv	TAGACAGGGCAGTAGACGGG	qRT-PCR
Irx5 fwd	AGCCCAAACTGTGGTCTCTG	qRT-PCR
Irx5 Rv	CACGGTGGGCATGGAGAG	qRT-PCR
Gata4 fwd	CTGTGGCCTCTATCACAAGATG	qRT-PCR
Gata4 rv	GTGGTGGTAGTCTGGCAGTTG	qRT-PCR
Snai2 fwd	TGAAGATGCACATTCGAACC	qRT-PCR
Snai2 rv	CAGTGAGGGCAAGAGAAAGG	qRT-PCR
Birc5 fwd	AAGAACTGGCCCTTCCTGG	qRT-PCR
Birc5 rv	TAAAGCAGAAAAAACACTGGGC	qRT-PCR
Sox2 fwd	CTCTGTGGTCAAGTCCGAGG	qRT-PCR
Sox2 rv	CTGATCATGTCCCGGAGGTC	qRT-PCR
Tbx5 fwd	AGCAGGGCATGGAAGGAATC	qRT-PCR
Tbx5 rv	ATCTCTGTGCCCACTTCGTG	qRT-PCR
Igf1 fwd	TTCAGTTCGTGTGTGGACCG	qRT-PCR
Igf1 rv	GTCGATAGGGACGGGGACTTC	qRT-PCR
Ccnd1 fwd	CGAGAAGTTGTGCATCTACACTG	qRT-PCR
Ccnd1 rv	GCATTTTGGAGAGGAAGTGTTC	qRT-PCR
Ki67 fwd	CCTTTGCTGTCCCCGAAGA	qRT-PCR
Ki67 rv	GGCTTCTCATCTGTTGCTTCCT	qRT-PCR
Nppb fwd	GAGTCCTTCGGTCTCAAGGC	qRT-PCR
Nppb rv	CAACTTCAGTGCGTTACAGC	qRT-PCR
Nppa fwd	GGTAGGATTGACAGGATTGGAG	qRT-PCR
Nppa rv	GCTTAGGATCTTTTGCGATCTG	qRT-PCR
Myh7 fwd	TGACGCAGGAGAGCATCAT	qRT-PCR
Myh7 rv	GAGTGCATTTAACTCAAAGTCCTTC	qRT-PCR
Serca2a fwd	TGGTGATATAGTGGAAATTGCTG	qRT-PCR
Serca2a rv	GAGTTGTAGACTTGATGGATGTCAA	qRT-PCR
Pln fwd	GCTCAAGGGCTGTGTACATG	qRT-PCR

Pln rv	CAGCCAACACAGCAAGATGT	qRT-PCR
Ppargc1a fwd	GTCATGTGACTGGGGACTGT	qRT-PCR
Ppargc1a rv	AACCAGAGCAGCACACTCTAT	qRT-PCR
Luciferase fwd	ATAACTGGTCCGCAGTGGTG	qRT-PCR
Luciferase rv	TAAGAAGAGGCCGCGTTACC	qRT-PCR
sg*Tbx20* fwd	TGGACATAAGCGCGGCGA	sgRNA qRT-PCR
sg*Myh6* fwd	GTTAAGGCCAAGGTCGTGTCC	sgRNA qRT-PCR
sg*Sav1* fwd	AGTCATCCCCTTGAACGAGA	sgRNA qRT-PCR
sgRNA universal reverse	ACCGACTCGGTGCCACTT	sgRNA qRT-PCR
Myh6 T7 fwd	AGGCACCCTTACCCCACATA	T7 endonuclease assay
Myh6 T7 rv	CAACCCCTTTCCCTAAGCCG	T7 endonuclease assay
Tbx20 T7 fwd	GTTTTGCGCAGTGGGCTTAC	T7 endonuclease assay
Tbx20 T7 rv	CTTTGATTCCAAGCGCAGGC	T7 endonuclease assay
Sav1 T7 fwd	GGCCATTTTACACTGACACAG	T7 endonuclease assay
Sav1 T7 rv	TGACCCCTTGTCCTCAGTTC	T7 endonuclease assay
Sav1 exon deletion fwd	AGCTGGAAACGTGACTGATCT	PCR
Sav1 exon deletion fwd	AAGCTTCAAGATGCTTATCCCTT	PCR
Sal1 Cas9 fwd	TATTAgtcgacgccaccATGGACTATAAGGACCACG	Myh6 transgenic cloning
MluI-HindIII Cas9 rv	TATTAaagcttacgcgtAGGCTGATCAGCGAGCTCTAGG	Myh6 transgenic cloning
U6 primer	GAGGGCCTATTTCCCATGATTC	Sequencing primer
sgRNA insert check	GACTATCATATGCTTACCGT	Sequencing primer
Sav1 fwd left mate read	GTTCAGAGTTCTACAGTCCGACGATCXXXXXXXXTGGCCATTTTACACTGACACA	DNA sequencing
Sav1 rv left mate read	TTCCTTGGCACCCGAGAATTCCAACTCTACTCGTTCCCAGCC	DNA sequencing
Tbx20 fwd left mate read	GTTCAGAGTTCTACAGTCCGACGATCXXXXXXXXTGCTCTAGTGGACTGGAGAG	DNA sequencing
Tbx20 rv left mate read	TTCCTTGGCACCCGAGAATTCCATCTCTGCTGCCTCCTTCT	DNA sequencing
Myh6 fwd left mate read	GTTCAGAGTTCTACAGTCCGACGATCXXXXXXXXGCCCACACCAGAAATGACA	DNA sequencing
Myh6 rv left mate read	TTCCTTGGCACCCGAGAATTCCAGTTTTCAGTTTCCGCAGTGAC	DNA sequencing
Sav1 fwd right mate read	GTTCAGAGTTCTACAGTCCGACGATCCATAGATCATAACACAAATACC	DNA sequencing
Sav1 rv right mate read	TTCCTTGGCACCCGAGAATTCCAXXXXXXXXGAGAAATCACTTTAAAATCTCA	DNA sequencing
Tbx20 fwd right made read	GTTCAGAGTTCTACAGTCCGACGATCGCCCAAGCCCCAGCTCTC	DNA sequencing
Tbx20 rv right made read	TTCCTTGGCACCCGAGAATTCCAXXXXXXXXGTCTTTCTCCCAGGACCGAATTCTG	DNA sequencing
Myh6 fwd right made read	GTTCAGAGTTCTACAGTCCGACGATCTGCTTCGTGCCTGATGAC	DNA sequencing
Myh6 rv right made read	TTCCTTGGCACCCGAGAATTCCAXXXXXXXXGAGCATCCCTTGGGTGACAC	DNA sequencing
Universal second PCR primer fw	AATGATACGGCGACCACCGAGATCTACACGTTCAGAGTTCTACAGTCCGA	DNA sequencing
Universal second PCR primer	CAAGCAGAAGACGGCATACGAGATNNNNN	DNA sequencing

rv	NGTGACTGGAGTTCCTTGGCACCCGAGAAT TCCA*	

*XXXXXXXX = Barcode sequences as described in Junker et al.[1]
*NNNNNN = index from Illumina TruSeq Small RNA Sample Prep Kit

Reference List

1. Junker JP, Noel ES, Guryev V, Peterson KA, Shah G, Huisken J, McMahon AP, Berezikov E, Bakkers J, van Oudenaarden A. Genome-wide rna tomography in the zebrafish embryo. *Cell*. 2014;159:662-675

Data Supplement III

Plasmids

1. **α-MHC-Cas9 targeting vector**
2. **AAV:ITR-U6-sgRNA(backbone)-pEFs-Rluc-WPRE-hGHpA-ITR**

Plasmid 1. α-MHC-Cas9 targeting vector

Elements

α–MHC promoter
3xFLAG-tag
NLS
Cas9
NLS

GAATTCTCTTACTATCAAAGGGAAACTGAGTCGTGCACCTGCAAAGTGGATGCTCTC
CCTAGACATCATGACTTTGTCTCTGGGGAGCCAGCACTGTGGAACTTCAGGTCTGAG
AGAGTAGGAGGCTCCCCTCAGCCTGAAGCTATGCAGATAGCCAGGGTTGAAAGGGGG
AAGGGAGAGCCTGGGATGGGAGCTTGTGTGTTGGAGGCAGGGGACAGATATTAAGCC
TGGAAGAGAAGGTGACCCTTACCCAGTTGTTCAACTCACCCTTCAGATTAAAAATAA
CTGAGGTAAGGGCCTGGGTAGGGGAGGTGGTGTGAGACGCTCCTGTCTCTCCTCTAT
CTGCCCATCGGCCCTTTGGGGAGGAGGAATGTGCCCAAGGACTAAAAAAAGGCCATG
GAGCCAGAGGGGCGAGGGCAACAGACCTTTCATGGGCAAACCTTGGGGCCCTGCTGT
CCTCCTGTCACCTCCAGAGCCAAGGGATCAAAGGAGGAGGAGCCAGGACAGGAGGGA
AGTGGGAGGGAGGGTCCCAGCAGAGGACTCCAAATTTAGGCAGCAGGCATATGGGAT
GGGATATAAAGGGGCTGGAGCACTGAGAGCTGTCAGAGATTTCTCCAACCCAGGTAA
GAGGGAGTTTCGGGTGGGGGCTCTTCACCCACACCAGACCTCTCCCCACCTAGAAGG
AAACTGCCTTTCCTGGAAGTGGGGTTCAGGCCGGTCAGAGATCTGACAGGGTGGCCT
TCCACCAGCCTGGGAAGTTCTCAGTGGCAGGAGGTTTCCACAAGAAACACTGGATGC
CCCTTCCCTTACGCTGTCTTCTCCATCTTCCTCCTGGGGATGCTCCTCCCCGTCTTG
GTTTATCTTGGCTCTTCGTCTTCAGCAAGATTTGCCCTGTGCTGTCCACTCCATCTT
TCTCTACTGTCTCCGTGCCTTGCCTTGCCTTCTTGCGTGTCCTTCCTTTCCACCCAT
TTCTCACTTCACCTTTTCTCCCCTTCTCATTTGTATTCATCCTTCCTTCCTTCCTTC
CTTCCTTCCTTCCTTCCTTCCTTCCTTCCTTTCTCCCTTCCTTCCTTCCTTCCTTCC
TTCCTTCCTTCCTTCCTTCCTGTGTCAGAGTGCTGAGAATCACACCTGGGGTTCCCA
CCCTTATGTAAACAATCTTCCAGTGAGCCACAGCTTCAGTGCTGCTGGGTGCTCTCT
TACCTTCCTCACCCCCTGGCTTGTCCTGTTCCATCCTGGTCAGGATCTCTAGATTGG
TCTCCCAGCCTCTGCTACTCCTCTTCCTGCCTGTTCCTCTCTCTGTCCAGCTGCGCC
ACTGTGGTGCCTCGTTCCAGCTGTGGTCCACATTCTTCAGGATTCTCTGAAAAGTTA
ACCAGGTGAGAATGTTTCCCCTGTAGACAGCAGATCACGATTCTCCCGGAAGTCAGG
CTTCCAGCCCTCTCTTTCTCTGCCCAGCTGCCCGGCACTCTTAGCAAACCTCAGGCA
CCCTTACCCCACATAGACCTCTGACAGAGAAGCAGGCACTTTACATGGAGTCCTGGT
GGGAGAGCCATAGGCTACGGTGTAAAAGAGGCAGGGAAGTGGTGGTGTAGGAAAGTC
AGGACTTCACATAGAAGCCTAGCCCACACCAGAAATGACAGACAGATCCCTCCTATC
TCCCCCATAAGAGTTTGACAGACAGATCCCTCCTATCTCCCCCATAAGAGTTTGA**GT**
CGACgccaccATGGACTATAAGGACCACGACGGAGACTACAAGGATCATGATATTGA
TTACAAAGACGATGACGATAAGATGGCCCCAAAGAAGAAGCGGAAGGTCGGTATCCA
CGGAGTCCCAGCAGCCGACAAGAAGTACAGCATCGGCCTGGACATCGGCACCAACTC
TGTGGGCTGGGCCGTGATCACCGACGAGTACAAGGTGCCCAGCAAGAAATTCAAGGT
GCTGGGCAACACCGACCGGCACAGCATCAAGAAGAACCTGATCGGAGCCCTGCTGTT
CGACAGCGGCGAAACAGCCGAGGCCACCCGGCTGAAGAGAACCGCCAGAAGAAGATA

CACCAGACGGAAGAACCGGATCTGCTATCTGCAAGAGATCTTCAGCAACGAGATGGC
CAAGGTGGACGACAGCTTCTTCCACAGACTGGAAGAGTCCTTCCTGGTGGAAGAGGA
TAAGAAGCACGAGCGGCACCCCATCTTCGGCAACATCGTGGACGAGGTGGCCTACCA
CGAGAAGTACCCCACCATCTACCACCTGAGAAAGAAACTGGTGGACAGCACCGACAA
GGCCGACCTGCGGCTGATCTATCTGGCCCTGGCCCACATGATCAAGTTCCGGGGCCA
CTTCCTGATCGAGGGCGACCTGAACCCCGACAACAGCGACGTGGACAAGCTGTTCAT
CCAGCTGGTGCAGACCTACAACCAGCTGTTCGAGGAAAACCCCATCAACGCCAGCGG
CGTGGACGCCAAGGCCATCCTGTCTGCCAGACTGAGCAAGAGCAGACGGCTGGAAAA
TCTGATCGCCCAGCTGCCCGGCGAGAAGAAGAATGGCCTGTTCGGAAACCTGATTGC
CCTGAGCCTGGGCCTGACCCCCAACTTCAAGAGCAACTTCGACCTGGCCGAGGATGC
CAAACTGCAGCTGAGCAAGGACACCTACGACGACGACCTGGACAACCTGCTGGCCCA
GATCGGCGACCAGTACGCCGACCTGTTTCTGGCCGCCAAGAACCTGTCCGACGCCAT
CCTGCTGAGCGACATCCTGAGAGTGAACACCGAGATCACCAAGGCCCCCCTGAGCGC
CTCTATGATCAAGAGATACGACGAGCACCACCAGGACCTGACCCTGCTGAAAGCTCT
CGTGCGGCAGCAGCTGCCTGAGAAGTACAAAGAGATTTTCTTCGACCAGAGCAAGAA
CGGCTACGCCGGCTACATTGACGGCGGAGCCAGCCAGGAAGAGTTCTACAAGTTCAT
CAAGCCCATCCTGGAAAAGATGGACGGCACCGAGGAACTGCTCGTGAAGCTGAACAG
AGAGGACCTGCTGCGGAAGCAGCGGACCTTCGACAACGGCAGCATCCCCCACCAGAT
CCACCTGGGAGAGCTGCACGCCATTCTGCGGCGGCAGGAAGATTTTTACCCATTCCT
GAAGGACAACCGGGAAAAGATCGAGAAGATCCTGACCTTCCGCATCCCCTACTACGT
GGGCCCTCTGGCCAGGGGAAACAGCAGATTCGCCTGGATGACCAGAAAGAGCGAGGA
AACCATCACCCCCTGGAACTTCGAGGAAGTGGTGGACAAGGGCGCTTCCGCCCAGAG
CTTCATCGAGCGGATGACCAACTTCGATAAGAACCTGCCCAACGAGAAGGTGCTGCC
CAAGCACAGCCTGCTGTACGAGTACTTCACCGTGTATAACGAGCTGACCAAAGTGAA
ATACGTGACCGAGGGAATGAGAAAGCCCGCCTTCCTGAGCGGCGAGCAGAAAAAGGC
CATCGTGGACCTGCTGTTCAAGACCAACCGGAAAGTGACCGTGAAGCAGCTGAAAGA
GGACTACTTCAAGAAAATCGAGTGCTTCGACTCCGTGGAAATCTCCGGCGTGGAAGA
TCGGTTCAACGCCTCCCTGGGCACATACCACGATCTGCTGAAAATTATCAAGGACAA
GGACTTCCTGGACAATGAGGAAAACGAGGACATTCTGGAAGATATCGTGCTGACCCT
GACACTGTTTGAGGACAGAGAGATGATCGAGGAACGGCTGAAAACCTATGCCCACCT
GTTCGACGACAAAGTGATGAAGCAGCTGAAGCGGCGGAGATACACCGGCTGGGGCAG
GCTGAGCCGGAAGCTGATCAACGGCATCCGGGACAAGCAGTCCGGCAAGACAATCCT
GGATTTCCTGAAGTCCGACGGCTTCGCCAACAGAAACTTCATGCAGCTGATCCACGA
CGACAGCCTGACCTTTAAAGAGGACATCCAGAAAGCCCAGGTGTCCGGCCAGGGCGA
TAGCCTGCACGAGCACATTGCCAATCTGGCCGGCAGCCCCGCCATTAAGAAGGGCAT
CCTGCAGACAGTGAAGGTGGTGGACGAGCTCGTGAAAGTGATGGGCCGGCACAAGCC
CGAGAACATCGTGATCGAAATGGCCAGAGAGAACCAGACCACCCAGAAGGGACAGAA
GAACAGCCGCGAGAGAATGAAGCGGATCGAAGAGGGCATCAAAGAGCTGGGCAGCCA
GATCCTGAAAGAACACCCCGTGGAAAACACCCAGCTGCAGAACGAGAAGCTGTACCT
GTACTACCTGCAGAATGGGCGGGATATGTACGTGGACCAGGAACTGGACATCAACCG
GCTGTCCGACTACGATGTGGACCATATCGTGCCTCAGAGCTTTCTGAAGGACGACTC
CATCGACAACAAGGTGCTGACCAGAAGCGACAAGAACCGGGGCAAGAGCGACAACGT
GCCCTCCGAAGAGGTCGTGAAGAAGATGAAGAACTACTGGCGGCAGCTGCTGAACGC
CAAGCTGATTACCCAGAGAAAGTTCGACAATCTGACCAAGGCCGAGAGAGGCGGCCT
GAGCGAACTGGATAAGGCCGGCTTCATCAAGAGACAGCTGGTGGAAACCCGGCAGAT
CACAAAGCACGTGGCACAGATCCTGGACTCCCGGATGAACACTAAGTACGACGAGAA
TGACAAGCTGATCCGGGAAGTGAAAGTGATCACCCTGAAGTCCAAGCTGGTGTCCGA
TTTCCGGAAGGATTTCCAGTTTTACAAAGTGCGCGAGATCAACAACTACCACCACGC
CCACGACGCCTACCTGAACGCCGTCGTGGGAACCGCCCTGATCAAAAAGTACCCTAA
GCTGGAAAGCGAGTTCGTGTACGGCGACTACAAGGTGTACGACGTGCGGAAGATGAT
CGCCAAGAGCGAGCAGGAAATCGGCAAGGCTACCGCCAAGTACTTCTTCTACAGCAA
CATCATGAACTTTTTCAAGACCGAGATTACCCTGGCCAACGGCGAGATCCGGAAGCG

GCCTCTGATCGAGACAAACGGCGAAACCGGGGAGATCGTGTGGGATAAGGGCCGGGA
TTTTGCCACCGTGCGGAAAGTGCTGAGCATGCCCCAAGTGAATATCGTGAAAAAGAC
CGAGGTGCAGACAGGCGGCTTCAGCAAAGAGTCTATCCTGCCCAAGAGGAACAGCGA
TAAGCTGATCGCCAGAAAGAAGGACTGGGACCCTAAGAAGTACGGCGGCTTCGACAG
CCCCACCGTGGCCTATTCTGTGCTGGTGGTGGCCAAAGTGGAAAAGGGCAAGTCCAA
GAAACTGAAGAGTGTGAAAGAGCTGCTGGGGATCACCATCATGGAAAGAAGCAGCTT
CGAGAAGAATCCCATCGACTTTCTGGAAGCCAAGGGCTACAAAGAAGTGAAAAAGGA
CCTGATCATCAAGCTGCCTAAGTACTCCCTGTTCGAGCTGGAAAACGGCCGGAAGAG
AATGCTGGCCTCTGCCGGCGAACTGCAGAAGGGAAACGAACTGGCCCTGCCCTCCAA
ATATGTGAACTTCCTGTACCTGGCCAGCCACTATGAGAAGCTGAAGGGCTCCCCCGA
GGATAATGAGCAGAAACAGCTGTTTGTGGAACAGCACAAGCACTACCTGGACGAGAT
CATCGAGCAGATCAGCGAGTTCTCCAAGAGAGTGATCCTGGCCGACGCTAATCTGGA
CAAAGTGCTGTCCGCCTACAACAAGCACCGGGATAAGCCCATCAGAGAGCAGGCCGA
GAATATCATCCACCTGTTTACCCTGACCAATCTGGGAGCCCCTGCCGCCTTCAAGTA
CTTTGACACCACCATCGACCGGAAGAGGTACACCAGCACCAAAGAGGTGCTGGACGC
CACCCTGATCCACCAGAGCATCACCGGCCTGTACGAGACACGGATCGACCTGTCTCA
GCTGGGAGGCGACAAAAGGCCGGCGGCCACGAAAAAGGCCGGCCAGGCAAAAAAGAA
AAAGtaagaattcCTAGAGCTCGCTGATCAGCCT**ACGCGT**AAGCTTGATGGGTGGCA
TCC

Plasmid 2: AAV:ITR-U6-sgRNA(backbone)-pEFs-Rluc-WPRE-hGHpA-ITR

Elements:

ITR
U6
*sgRNA insert site
SapI restriction site
sgRNA + TracrRNA
EFs
Rluc
WPRE
hGHpA
ITR
Ampicillin promoter
Ampicillin
pBR322 origin
Restriction sites; separated by *, for cloning dual sgRNA

CCTGCAGGCAGCTGCGCGCTCGCTCGCTCACTGAGGCCGCCCGGGCAAAGCCCGGGC
GTCGGGCGACCTTTGGTCGCCCGGCCTCAGTGAGCGAGCGAGCGCGCAGAGAGGGAG
TGGCCAACTCCATCACTAGGGGTTCCTgcggccgcacgcgtGAGGGCCTATTTCCCA
TGATTCCTTCATATTTGCATATACGATACAAGGCTGTTAGAGAGATAATTGGAATTA
ATTTGACTGTAAACACAAAGATATTAGTACAAAATACGTGACGTAGAAAGTAATAAT
TTCTTGGGTAGTTTGCAGTTTTAAAATTATGTTTTAAAATGGACTATCATATGCTTA
CCGTAACTTGAAAGTATTTCGATTTCTTGGCTTTATATATCTTGTGGAAAGGACGAA
ACACCGGAAGAGCGACGCTCTTCT*GTTTTAGAGCTAGAAATAGCAAGTTAAAATAAG
GCTAGTCCGTTATCAACTTGAAAAAGTGGCACCGAGTCGGTGCTTTTTTtctaga*g
gtaccAGGTCTTGAAAGGAGTGGGAATTGGCTCCGGTGCCCGTCAGTGGGCAGAGCG
CACATCGCCCACAGTCCCCGAGAAGTTGGGGGGAGGGGTCGGCAATTGAACCGGTGC

CTAGAGAAGGTGGCGCGGGGTAAACTGGGAAAGTGATGTCGTGTACTGGCTCCGCCT
TTTTCCCGAGGGTGGGGGAGAACCGTATATAAGTGCAGTAGTCGCCGTGAACGTTCT
TTTTCGCAACGGGTTTGCCGCCAGAACACAGGCGTACGGCCACCATGACTTCGAAAG
TTTATGATCCAGAACAAAGGAAACGGATGATAACTGGTCCGCAGTGGTGGGCCAGAT
GTAAACAAATGAATGTTCTTGATTCATTTATTAATTATTATGATTCAGAAAAACATG
CAGAAAATGCTGTTATTTTTTTACATGGTAACGCGGCCTCTTCTTATTTATGGCGAC
ATGTTGTGCCACATATTGAGCCAGTAGCGCGGTGTATTATACCAGACCTTATTGGTA
TGGGCAAATCAGGCAAATCTGGTAATGGTTCTTATAGGTTACTTGATCATTACAAAT
ATCTTACTGCATGGTTTGAACTTCTTAATTTACCAAAGAAGATCATTTTTGTCGGCC
ATGATTGGGGTGCTTGTTTGGCATTTCATTATAGCTATGAGCATCAAGATAAGATCA
AAGCAATAGTTCACGCTGAAAGTGTAGTAGATGTGATTGAATCATGGGATGAATGGC
CTGATATTGAAGAAGATATTGCGTTGATCAAATCTGAAGAAGGAGAAAAAATGGTTT
TGGAGAATAACTTCTTCGTGGAAACCATGTTGCCATCAAAAATCATGAGAAAGTTAG
AACCAGAAGAATTTGCAGCATATCTTGAACCATTCAAAGAGAAAGGTGAAGTTCGTC
GTCCAACATTATCATGGCCTCGTGAAATCCCGTTAGTAAAAGGTGGTAAACCTGACG
TTGTACAAATTGTTAGGAATTATAATGCTTATCTACGTGCAAGTGATGATTTACCAA
AAATGTTTATTGAATCGGACCCAGGATTCTTTTCCAATGCTATTGTTGAAGGTGCCA
AGAAGTTTCCTAATACTGAATTTGTCAAAGTAAAAGGTCTTCATTTTTCGCAAGAAG
ATGCACCTGATGAAATGGGAAAATATATCAAATCGTTCGTTGAGCGAGTTCTCAAAA
ATGAACAAGCTAGCGGAAGCGGAGGATATCAAGCTTATCGATAATCAACCTCTGGAT
TACAAAATTTGTGAAAGATTGACTGGTATTCTTAACTATGTTGCTCCTTTTACGCTA
TGTGGATACGCTGCTTTAATGCCTTTGTATCATGCTATTGCTTCCCGTATGGCTTTC
ATTTTCTCCTCCTTGTATAAATCCTGGTTGCTGTCTCTTTATGAGGAGTTGTGGCCC
GTTGTCAGGCAACGTGGCGTGGTGTGCACTGTGTTTGCTGACGCAACCCCCACTGGT
TGGGGCATTGCCACCACCTGTCAGCTCCTTTCCGGGACTTTCGCTTTCCCCCTCCCT
ATTGCCACGGCGGAACTCATCGCCGCCTGCCTTGCCCGCTGCTGGACAGGGGCTCGG
CTGTTGGGCACTGACAATTCCGTGGTGTTGTCGGGGAAATCATCGTCCTTTCCTTGG
CTGCTCGCCTATGTTGCCACCTGGATTCTGCGCGGGACGTCCTTCTGCTACGTCCCT
TCGGCCCTCAATCCAGCGGACCTTCCTTCCCGCGGCCTGCTGCCGGCTCTGCGGCCT
CTTCCGCGTCTTCGCCTTCGCCCTCAGACGAGTCGGATCTCCCTTTGGGCCGCCTCC
CCGCATCGATACCGAGCGCTGCTCGAGAGATCTACGGGTGGCATCCCTGTGACCCCT
CCCCAGTGCCTCTCCTGGCCCTGGAAGTTGCCACTCCAGTGCCCACCAGCCTTGTCC
TAATAAAATTAAGTTGCATCATTTTGTCTGACTAGGTGTCCTTCTATAATATTATGG
GGTGGAGGGGGGTGGTATGGAGCAAGGGGCAAGTTGGGAAGACAACCTGTAGGGCCT
GCGGGGTCTATTGGGAACCAAGCTGGAGTGCAGTGGCACAATCTTGGCTCACTGCAA
TCTCCGCCTCCTGGGTTCAAGCGATTCTCCTGCCTCAGCCTCCCGAGTTGTTGGGAT
TCCAGGCATGCATGACCAGGCTCAGCTAATTTTTGTTTTTTTGGTAGAGACGGGGTT
TCACCATATTGGCCAGGCTGGTCTCCAACTCCTAATCTCAGGTGATCTACCCACCTT
GGCCTCCCAAATTGCTGGGATTACAGGCGTGAACCACTGCTCCCTTCCCTGTCCTTC
TGATTTTGTAGGTAACCACGTGCGGACCGAGCGGCCGCAGGAACCCCTAGTGATGGA
GTTGGCCACTCCCTCTCTGCGCGCTCGCTCGCTCACTGAGGCCGGGCGACCAAAGGT
CGCCCGACGCCCGGGCTTTGCCCGGGCGGCCTCAGTGAGCGAGCGAGCGCGCAGCTG
CCTGCAGGGGCGCCTGATGCGGTATTTTCTCCTTACGCATCTGTGCGGTATTTCACA
CCGCATACGTCAAAGCAACCATAGTACGCGCCCTGTAGCGGCGCATTAAGCGCGGCG
GGTGTGGTGGTTACGCGCAGCGTGACCGCTACACTTGCCAGCGCCCTAGCGCCCGCT
CCTTTCGCTTTCTTCCCTTCCTTTCTCGCCACGTTCGCCGGCTTTCCCCGTCAAGCT
CTAAATCGGGGGCTCCCTTTAGGGTTCCGATTTAGTGCTTTACGGCACCTCGACCCC
AAAAAACTTGATTTGGGTGATGGTTCACGTAGTGGGCCATCGCCCTGATAGACGGTT
TTTCGCCCTTTGACGTTGGAGTCCACGTTCTTTAATAGTGGACTCTTGTTCCAAACT
GGAACAACACTCAACCCTATCTCGGGCTATTCTTTTGATTTATAAGGGATTTTGCCG
ATTTCGGCCTATTGGTTAAAAAATGAGCTGATTTAACAAAAATTTAACGCGAATTTT
AACAAAATATTAACGTTTACAATTTTATGGTGCACTCTCAGTACAATCTGCTCTGAT

GCCGCATAGTTAAGCCAGCCCCGACACCCGCCAACACCCGCTGACGCGCCCTGACGG
GCTTGTCTGCTCCCGGCATCCGCTTACAGACAAGCTGTGACCGTCTCCGGGAGCTGC
ATGTGTCAGAGGTTTTCACCGTCATCACCGAAACGCGCGAGACGAAAGGGCCTCGTG
ATACGCCTATTTTTATAGGTTAATGTCATGATAATAATGGTTTCTTAGACGTCAGGT
GGCACTTTTCGGGGAAATGTGCGCGGAACCCCTATTTGTTTATTTTTCTAAATACAT
TCAAATATGTATCCGCTCATGAGACAATAACCCTGATAAATGCTTCAATAATATTGA
AAAAGGAAGAGTATGAGTATTCAACATTTCCGTGTCGCCCTTATTCCCTTTTTTGCG
GCATTTTGCCTTCCTGTTTTTGCTCACCCAGAAACGCTGGTGAAAGTAAAAGATGCT
GAAGATCAGTTGGGTGCACGAGTGGGTTACATCGAACTGGATCTCAACAGCGGTAAG
ATCCTTGAGAGTTTTCGCCCCGAAGAACGTTTTCCAATGATGAGCACTTTTAAAGTT
CTGCTATGTGGCGCGGTATTATCCCGTATTGACGCCGGGCAAGAGCAACTCGGTCGC
CGCATACACTATTCTCAGAATGACTTGGTTGAGTACTCACCAGTCACAGAAAAGCAT
CTTACGGATGGCATGACAGTAAGAGAATTATGCAGTGCTGCCATAACCATGAGTGAT
AACACTGCGGCCAACTTACTTCTGACAACGATCGGAGGACCGAAGGAGCTAACCGCT
TTTTTGCACAACATGGGGGATCATGTAACTCGCCTTGATCGTTGGGAACCGGAGCTG
AATGAAGCCATACCAAACGACGAGCGTGACACCACGATGCCTGTAGCAATGGCAACA
ACGTTGCGCAAACTATTAACTGGCGAACTACTTACTCTAGCTTCCCGGCAACAATTA
ATAGACTGGATGGAGGCGGATAAAGTTGCAGGACCACTTCTGCGCTCGGCCCTTCCG
GCTGGCTGGTTTATTGCTGATAAATCTGGAGCCGGTGAGCGTGGGTCTCGCGGTATC
ATTGCAGCACTGGGGCCAGATGGTAAGCCCTCCCGTATCGTAGTTATCTACACGACG
GGGAGTCAGGCAACTATGGATGAACGAAATAGACAGATCGCTGAGATAGGTGCCTCA
CTGATTAAGCATTGGTAACTGTCAGACCAAGTTTACTCATATATACTTTAGATTGAT
TTAAAACTTCATTTTTAATTTAAAAGGATCTAGGTGAAGATCCTTTTTGATAATCTC
ATGACCAAAATCCCTTAACGTGAGTTTTCGTTCCACTGAGCGTCAGACCCCGTAGAA
AAGATCAAAGGATCTTCTTGAGATCCTTTTTTTCTGCGCGTAATCTGCTGCTTGCAA
ACAAAAAAACCACCGCTACCAGCGGTGGTTTGTTTGCCGGATCAAGAGCTACCAACT
CTTTTTCCGAAGGTAACTGGCTTCAGCAGAGCGCAGATACCAAATACTGTCCTTCTA
GTGTAGCCGTAGTTAGGCCACCACTTCAAGAACTCTGTAGCACCGCCTACATACCTC
GCTCTGCTAATCCTGTTACCAGTGGCTGCTGCCAGTGGCGATAAGTCGTGTCTTACC
GGGTTGGACTCAAGACGATAGTTACCGGATAAGGCGCAGCGGTCGGGCTGAACGGGG
GGTTCGTGCACACAGCCCAGCTTGGAGCGAACGACCTACACCGAACTGAGATACCTA
CAGCGTGAGCTATGAGAAAGCGCCACGCTTCCCGAAGGGAGAAAGGCGGACAGGTAT
CCGGTAAGCGGCAGGGTCGGAACAGGAGAGCGCACGAGGGAGCTTCCAGGGGGAAAC
GCCTGGTATCTTTATAGTCCTGTCGGGTTTCGCCACCTCTGACTTGAGCGTCGATTT
TTGTGATGCTCGTCAGGGGGGCGGAGCCTATGGAAAAACGCCAGCAACGCGGCCTTT
TTACGGTTCCTGGCCTTTTGCTGGCCTTTTGCTCACATGT

Supplemental Material - Online Figure I

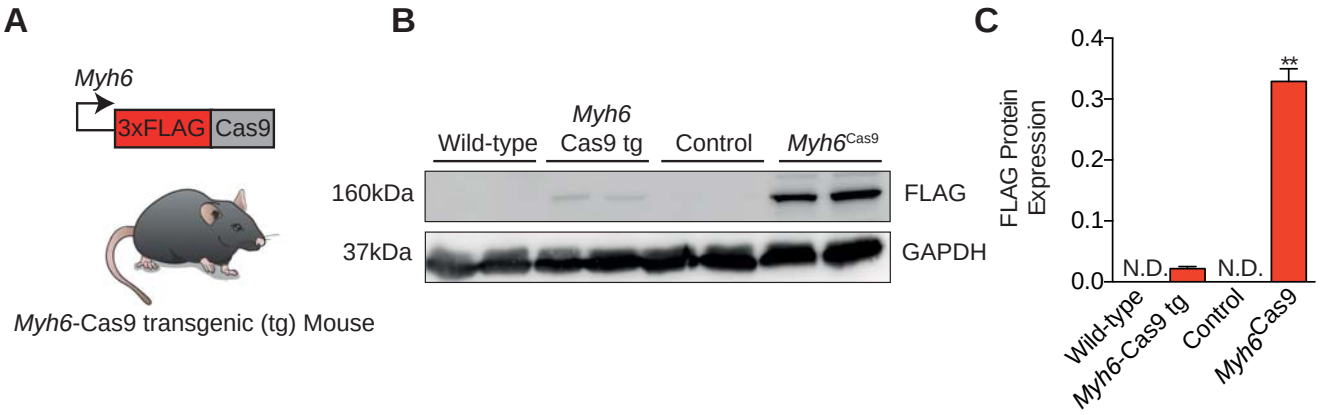

Online Figure I. Generation of cardiomyocyte-specific Cas9 expressing mice. (**A**) Strategy for the generation of *Myh6*-Cas9 transgenic (tg) (cardiomyocyte restricted) mice. (**B**) Western blot for FLAG (Cas9) expression in wild-type, Myh6-Cas9 tg (f1 generation), control (R26-lsl-3xFLAG-P2A-eGFP) and *Myh6*^{Cas9} mice. (**C**) Quantification of immunoblot in **B**. Data is represented as the mean ± SEM. N.D.; not detected. **P<0.01. n=2 mice per group.

Online Figure II

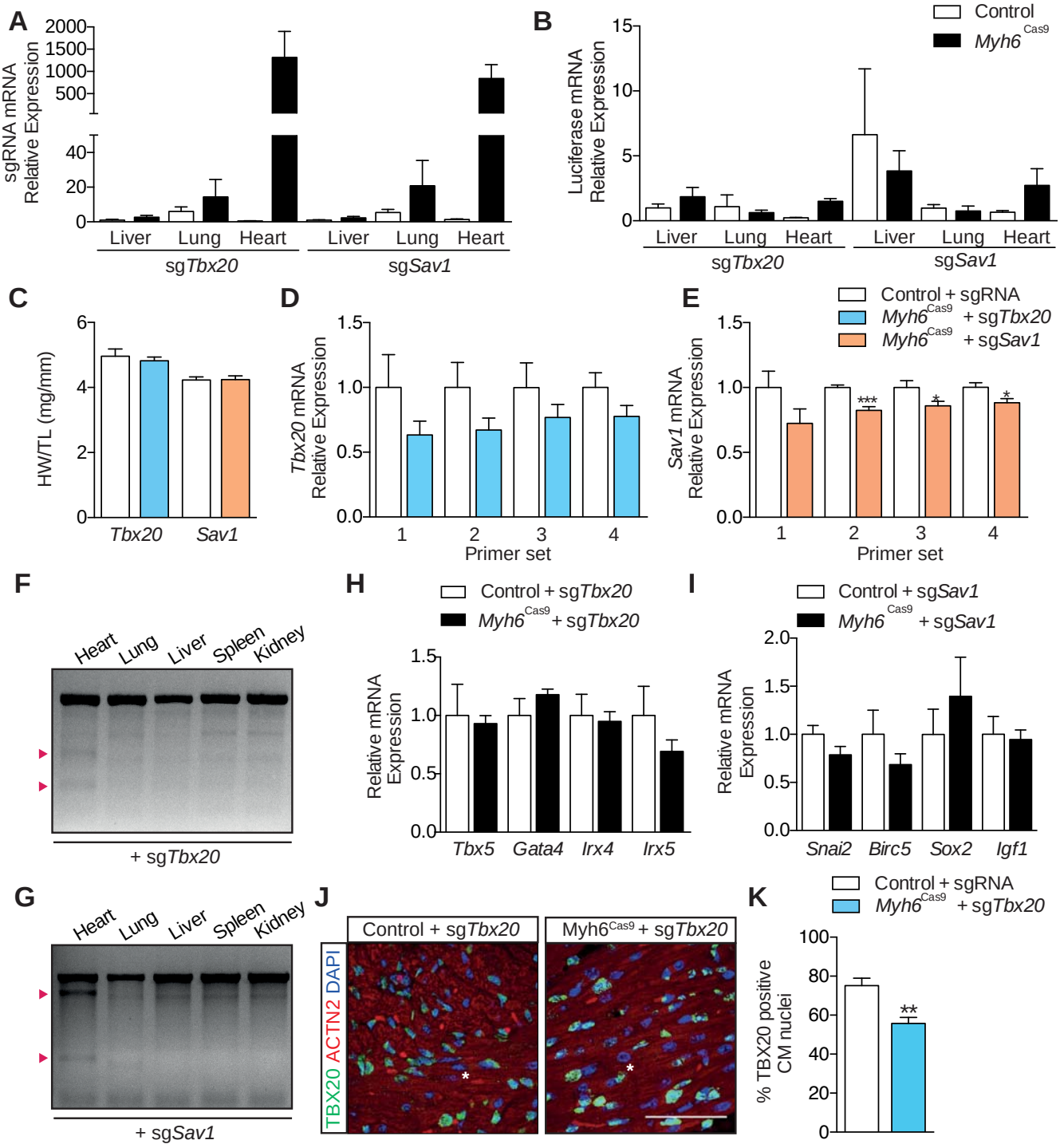

Online Figure II. ***In vivo*** **genome editing in the heart of a cardiomyocyte-specific Cas9 mouse.** Mice were injected with either AAV9-sg*Tbx20* or -sg*Sav1* at P3 by i.p. injection at a dose of $5x10^{11}$ viral genomes and analyzed 2 weeks later. (**A**) sgRNA and (**B**) Luciferase expression was measured by qRT-PCR analysis in the liver, lung and heart of sgRNA injected mice. (**C**) Heart weight/tibia length (HW/TL) of sgRNA injected mice. (**D-E**) qRT-PCR analysis of Tbx20 (**D**) and Sav1 (**E**) mRNA expression using different primer pairs. (**F-G**) T7E1 analysis on target site of PCR-amplified genomic DNA from isolated heart, lung, liver, spleen and kidney from *Myh6*^{Cas9} mice for (**E**) *Tbx20* and (**F**) *Sav1* to assess cardiac-restricted Cas9 expression. Red arrowheads indicate cut bands by T7E1 (**H-I**) The effect of cardiac gene disruption on known downstream targets of (**H**) Tbx20 and (**I**) Sav1. T-box 5 (Tbx5); gata-binding factor 4 (*Gata4*); Iroquois homeobox 4/5 (*Irx4/5*); snail family zinc finger 2 (*Snai2*); sex determining region Y-box 2 (*Sox2*); insulin-like growth factor (*Igf1*). Data was normalized to Gapdh. n=4-10 mice per group. (**J-K**) Immunoflouresnece detection (**J**) and quantification (**K**) of TBX20 expression in *Tbx20*-edited mice. Scale bar is 50μm. Data is represented as the mean ± SEM.

Online Figure III

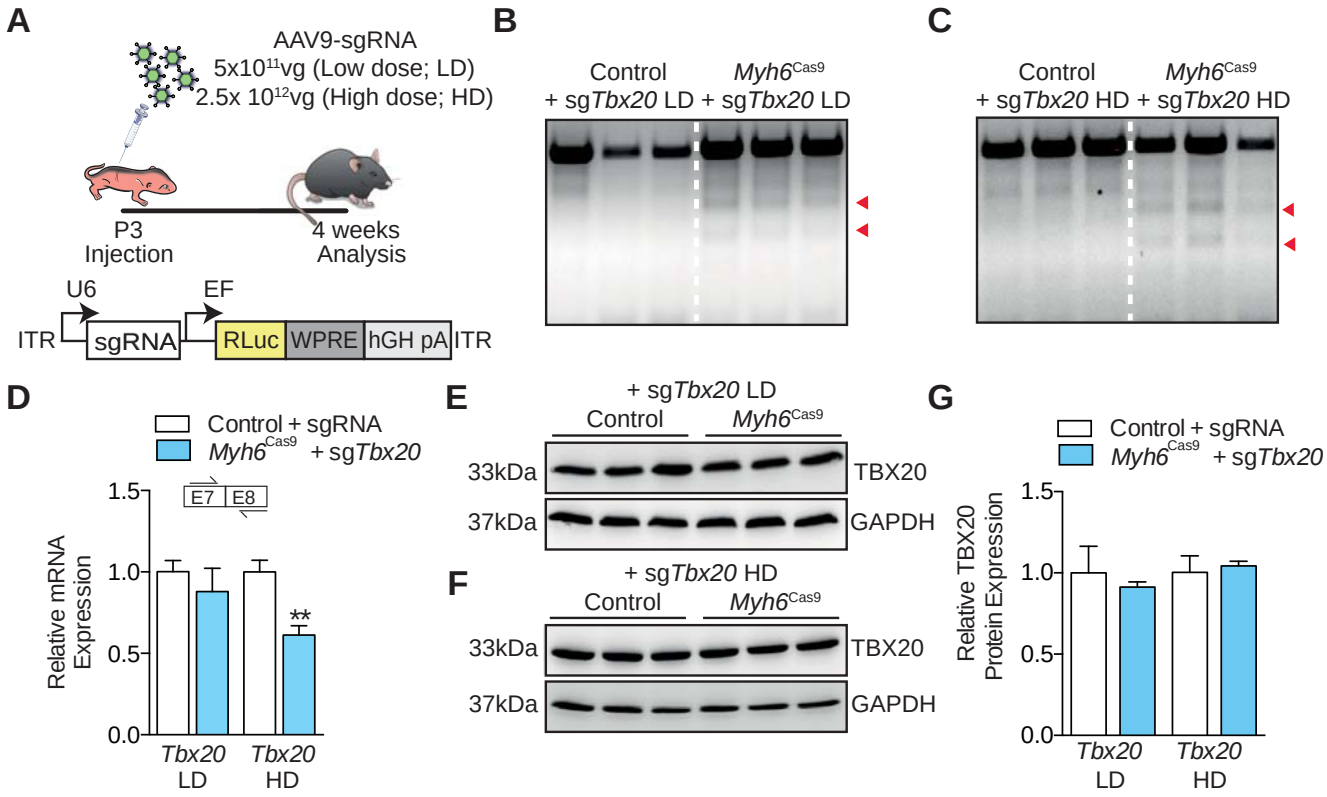

Online Figure III. Effect of viral dose on cardiac-genome editing *in vivo* using CRISPR/Cas9. (**A**) Schematic of study outline and sgRNA vector incorporated into AAV9. (**B-C**) T7E1 analysis on target site of PCR-amplified genomic DNA from isolated hearts from sg*Tbx20* low dose (LD) (**B**) and high dose (HD) (**C**). Red arrowheads indicate cut bands by T7E1 (**D**) Cardiac *Tbx20* mRNA analysis by qRT-PCR and (**E-G**) representative Western blot and quantification for cardiac TBX20 expression. GAPDH was used as the loading control. Data is represented as the mean ± SEM. **P<0.01. n=2-5 mice per group.

Online Figure IV

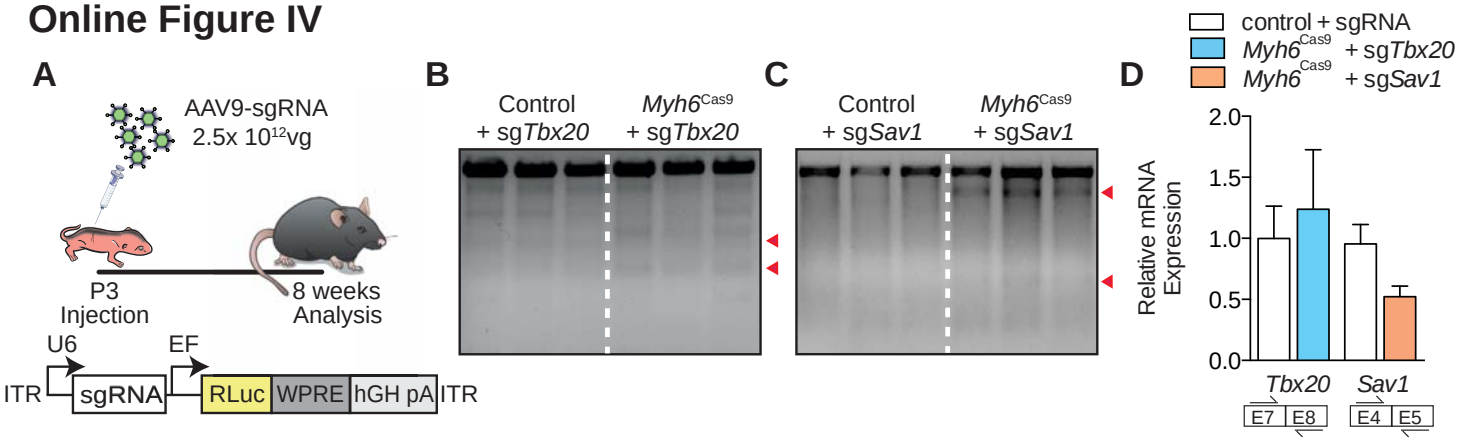

Online Figure IV. Long-term effect of cardiac-genome editing *in vivo* using CRISPR/Cas9. (**A**) Schematic of study outline and sgRNA vector incorporated into AAV9. (**B-C**) T7E1 analysis on target site of PCR-amplified genomic DNA from isolated hearts for *Tbx20* (**B**) and *Sav1* (**C**). Red arrowheads indicate cut bands by T7E1 (**D**) qRT-PCR analysis of cardiac *Tbx20* and *Sav1* mRNA. Data was normalized to *Gapdh*. Data is represented as the mean ± SEM. n=4-6 mice per group.

Online Figure V

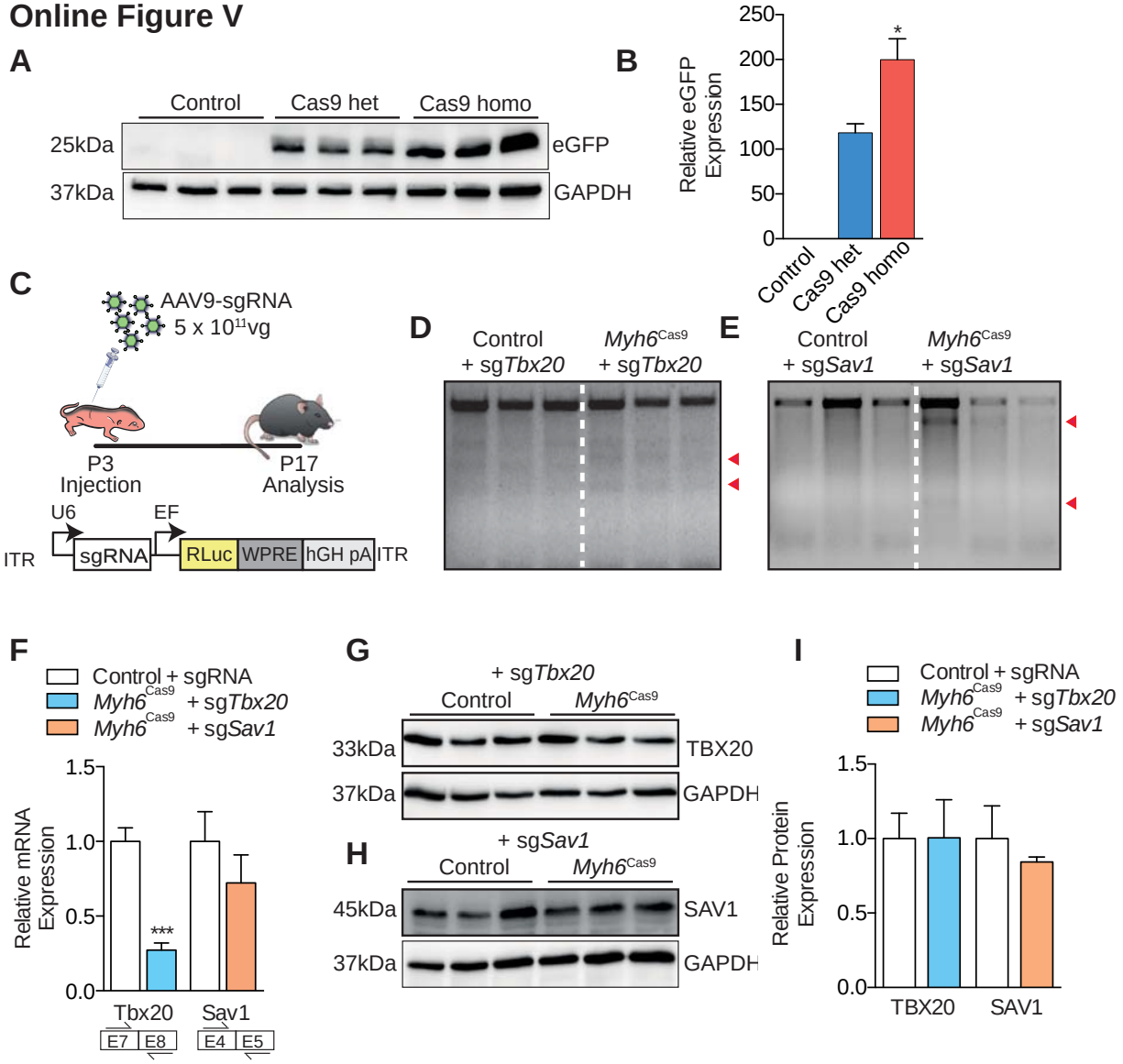

Online Figure V. Effect of Cas9 expression on cardiac-genome editing *in vivo* using CRISPR/Cas9. (**A**) Western blot analysis and (**B**) quantification of eGFP (Cas9) expression in control, heterozygous (het) and homozygous (homo) *Myh6*^{Cas9} mice. (**C**) Schematic of study outline and sgRNA vector incorporated into AAV9. (**D-E**) T7E1 analysis on target site of PCR-amplified genomic DNA from isolated hearts for *Tbx20* (**D**) and *Sav1* (**E**). Red arrowheads indicate cut bands by T7E1. (**F**) qRT-PCR analysis of cardiac *Tbx20* and *Sav1* mRNA. Data was normalized to *Gapdh*. (**G-I**) Representative Western blot and quantification for cardiac TBX20 and SAV1 expression. GAPDH was used as the loading control. Data is represented as the mean ± SEM. *P<0.05, **P<0.01, ***P<0.001. n=3-5 mice per group.

Online Figure VI

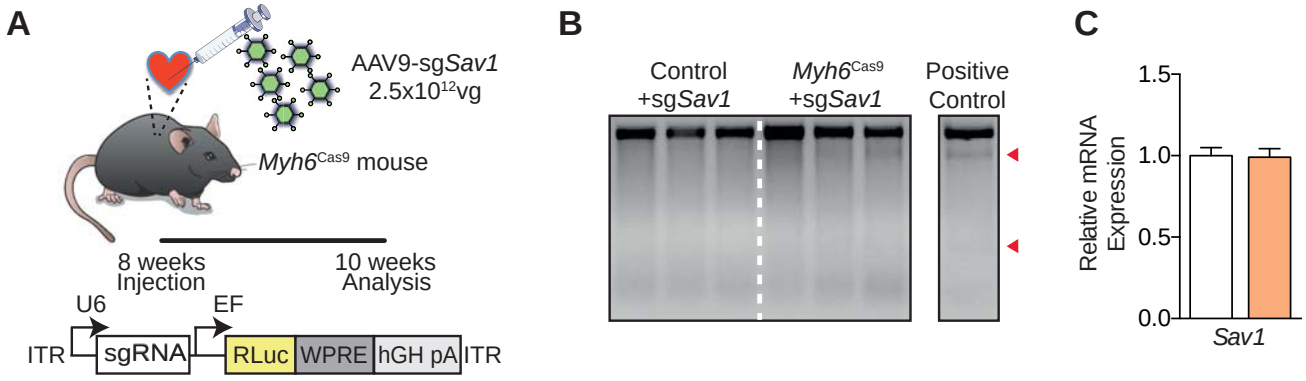

Online Figure VI. *In Vivo* genome editing of the heart by local delivery of sgRNAs using AAV9. (**A**) Schematic of study outline and sgRNA vector incorporated into AAV9. (**B**) T7E1 analysis on target site of PCR-amplified genomic DNA from isolated hearts for *Sav1*. Red arrowheads indicate cut bands by T7E1. (**C**) *Sav1* mRNA analysis by qRT-PCR on left ventricular samples isolated from the injected site. Data was normalized to *Gapdh*. n=5-7 mice per group. vg; viral genomes.

Online Figure VII

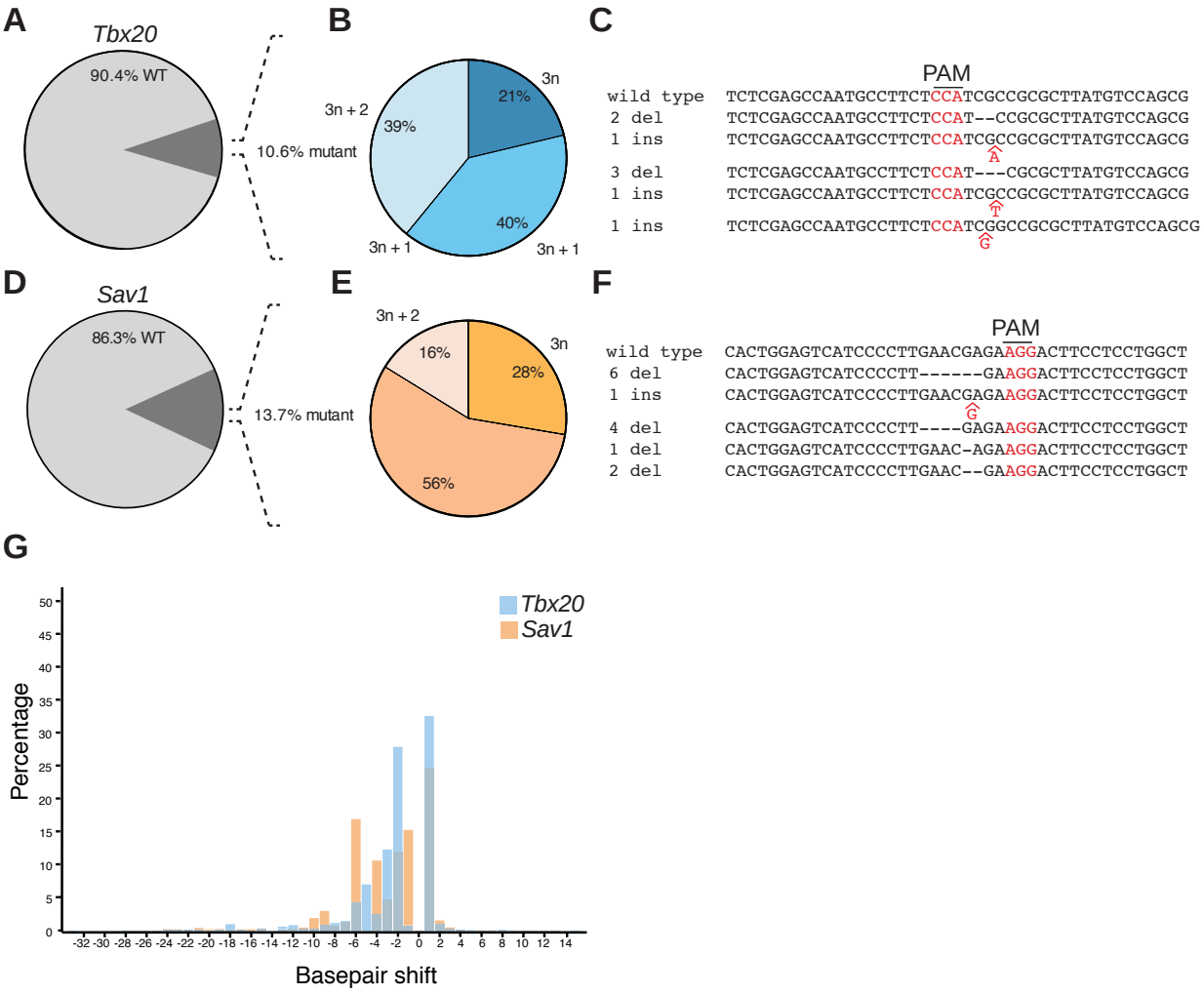

Online Figure VII. In-depth indel analysis of *in vivo Tbx20* and *Sav1* cardio-editing by DNA sequencing using a second primer set. Deep sequencing analysis of the *Tbx20* and *Sav1* locus of hearts isolated at P17 from mice injected with an sgRNA at P3 (from Figure 3A) using a second primer set, with the barcode primer located in the forward primer (**A**) Percentage of mutant reads in AAV9-sg*Tbx20* injected *Myh6*^{Cas9} mice and (**B**) the corresponding indel analysis and (**C**) the most abundant sequencing reads. (**D**) Percentage of mutant reads in AAV9-sg*Sav1* injected *Myh6*^{Cas9} mice and (**E**) the corresponding indel analysis and (**F**) the most abundant sequencing reads. (**G**) Size distribution of indels found at each sgRNA targeting site. Data is the average of 4 mice.

Online Figure VIII

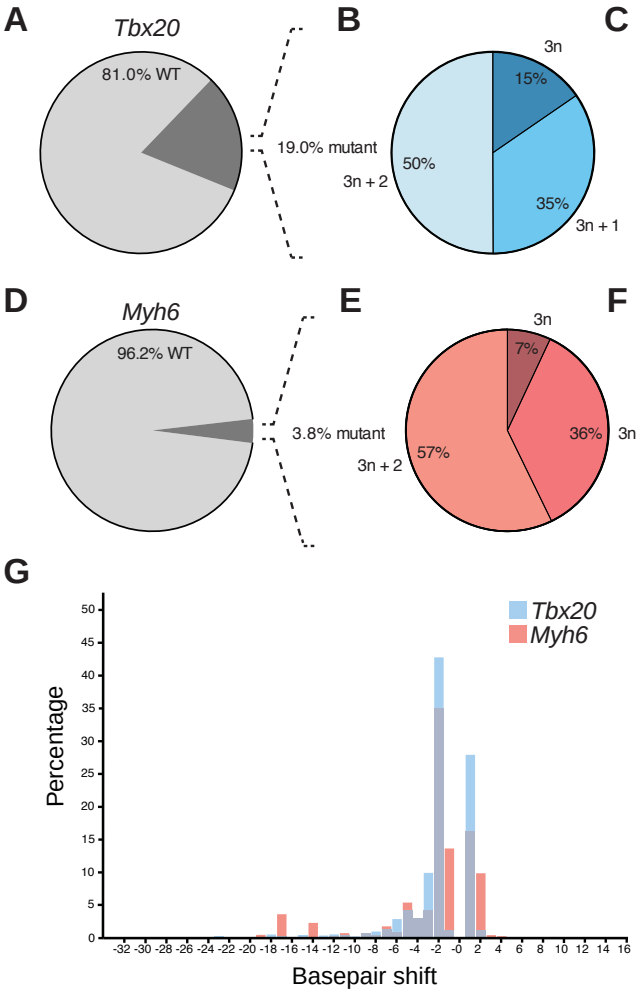

Online Figure VIII. In-depth indel analysis of *in vivo Tbx20* and *Myh6* cardio-editing by DNA sequencing using a second primer set. Deep sequencing analysis of the *Tbx20* and *Myh6* locus of hearts isolated at 5-6 weeks of age from mice injected with an sgRNA at P10 (from Figure 5A) using a second primer set, with the barcode primer located in the forward primer. (**A**) Percentage of mutant reads in AAV9-sg*Tbx20* injected *Myh6*^{Cas9} mice and (**B**) the corresponding indel analysis and (**C**) the most abundant sequencing reads. (**D**) Percentage of mutant reads in AAV9-sg*Myh6* injected *Myh6*^{Cas9} mice and (**E**) the corresponding indel analysis and (**F**) the most abundant sequencing reads. (**G**) Size distribution of indels found at each sgRNA targeting site. Data is the average of 3-4 mice.

Online Figure IX

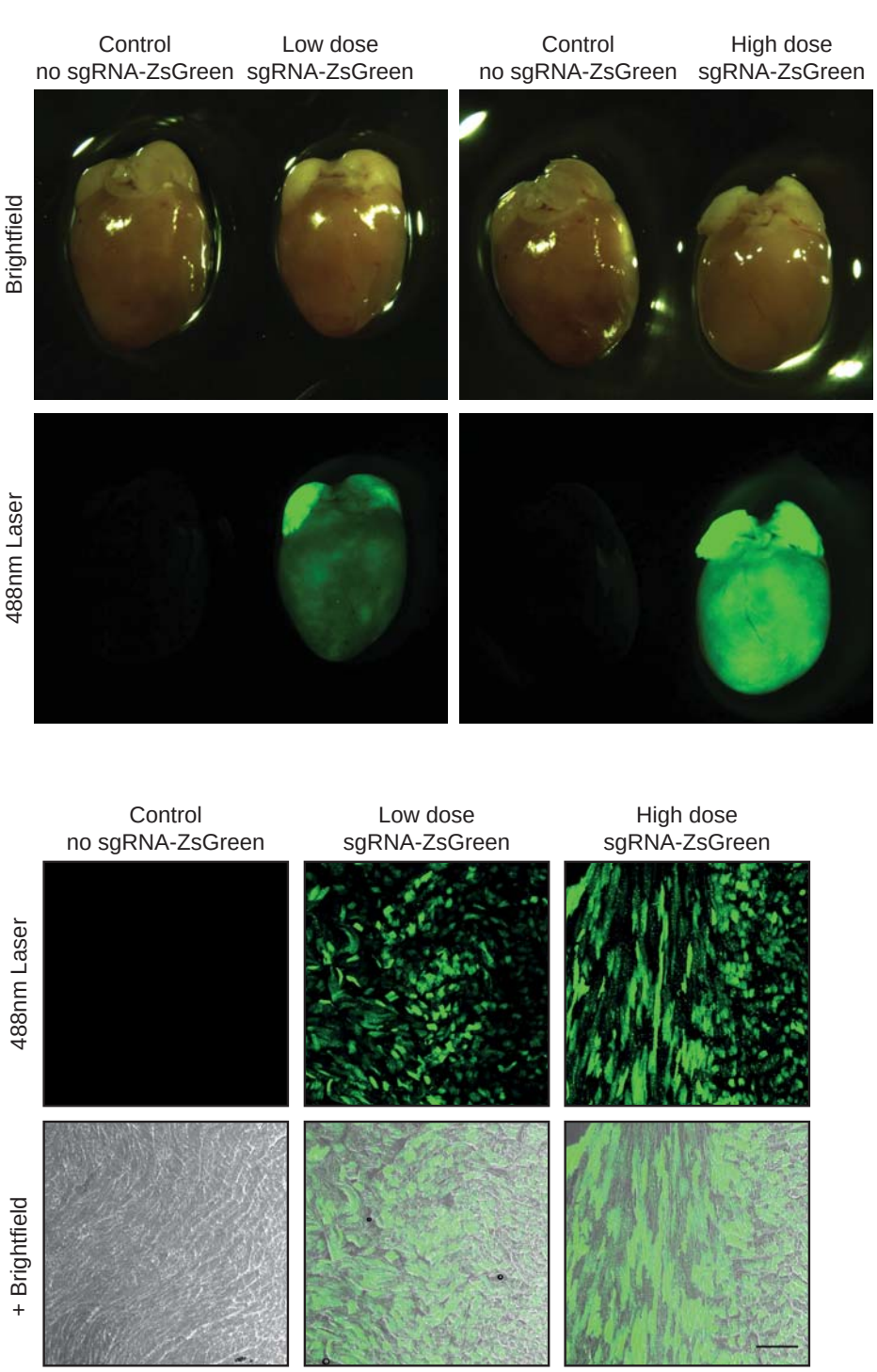

Online Figure IX. Cardiac tracing of sgRNA delivery by AAV9 low and high dose. Wild type mice were injected at P3 with either a low (5 x10^{11}vg per mouse) or a high (2.5 x10^{12}vg per mouse) dose of AAV9-sgRNA-Zsgreen by i.p. injection and analyzed two weeks later. (**A**) Representative stereomicroscope imaging of whole hearts from uninjected and injected hearts. (**B**) Confocal imaging of fixed and frozen heart sections. Image is taken in the left ventricle. Scale bar is 100μm. A total of 4 mice were analyzed per group, which all showed very similar results within groups.

Online Figure V

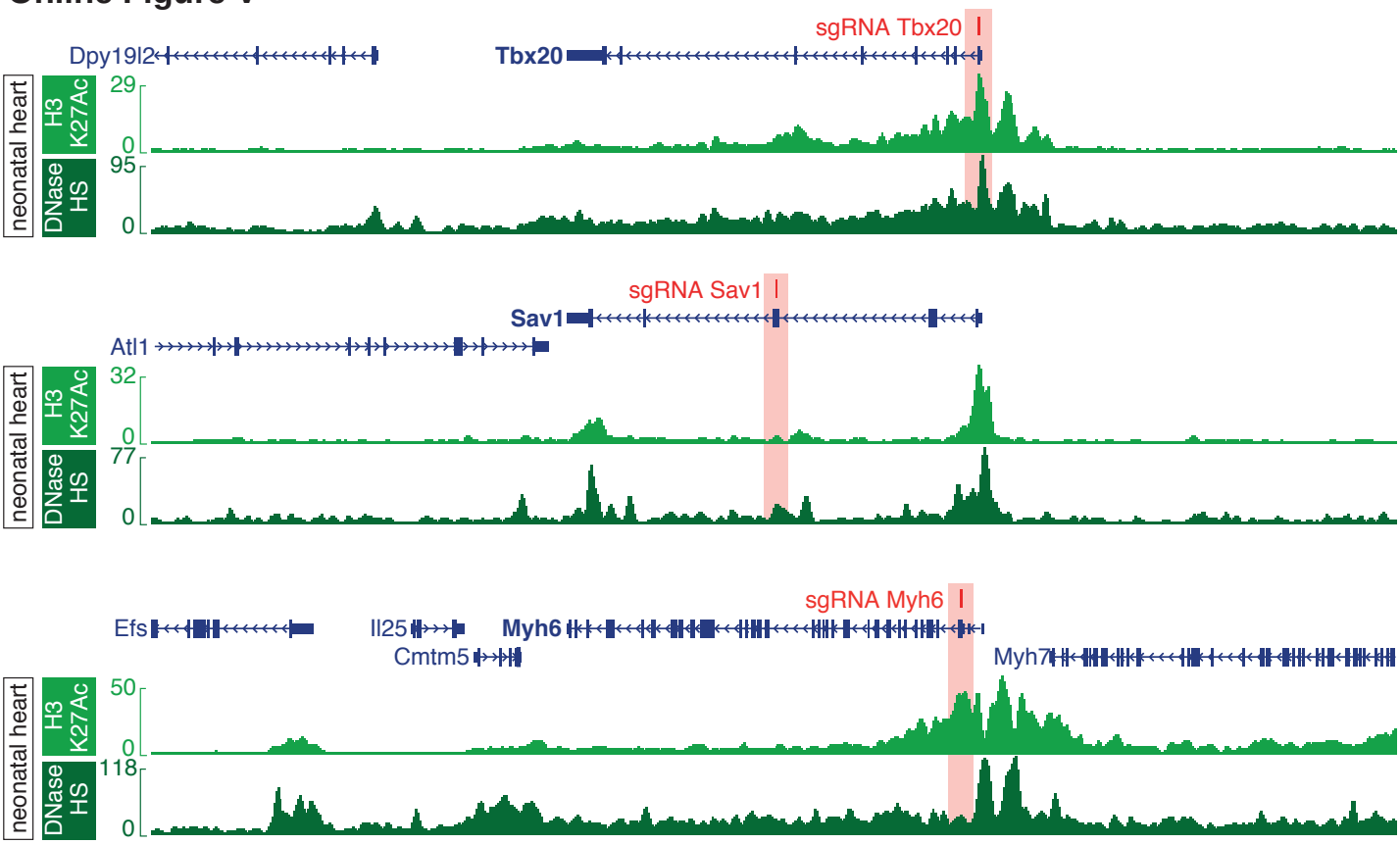

Online Figure V. Chromatin accessibility of targeted genomic loci. The active enhancer mark, H3k27Ac and DNase-Seq hotspots at the sgRNA targeted locus for each gene in neonatal mouse hearts from publicly available Chip-seq databases[33].